Ly49Q^{lo} RAW264 cells were analyzed, and the same results were obtained (data not shown). Ly49Q^{hi} and Ly49Q^{lo} RAW264 clones showed comparable expression levels of CD11b, F4/80, TLR4, and TLR9 (supplemental Figures 2A, 3B). To confirm the importance of Ly49Q in TLR9 signaling in RAW264 cells, Ly49Q^{hi} or Ly49Q^{lo} RAW264 cells were treated with CpG, and the TLR9-triggered cytokine production was examined. When the cells were stimulated with CpG, the Ly49Q^{hi} RAW264 cells produced IFN-β and IL-6, and the Ly49Q^{lo} RAW264 cells produced little, if any (Figure 3C and supplemental Figure 2B). These results were consistent with our findings that pDCs in Ly49Q$^{-/-}$ mice show impaired TLR9-mediated type I IFN production and that Ly49Q^{-} pDCs from bone marrow are less potent producers of IFN-β and IL-6 (Figure 2E).[10] In addition, the Ly49Q^{hi} and Ly49Q^{lo} RAW264 cells were morphologically different in their spreading and adhesion properties and in their formation of cytoplasmic vacuolar structures in the presence of CpG (supplemental Figure 2C). When exogenous Ly49Q-WT was expressed in Ly49Q^{lo} RAW264 cells, the CpG-induced IL-6 production recovered (supplemental Figure 2D-E). However, the ITIM-less mutant (Ly49Q-YF) did not rescue the IL-6 production efficiently, indicating that the ITIM is important for TLR9 signaling.

To further confirm that the effects in the Ly49Q^{lo} RAW264 cells were due to the decreased Ly49Q and not to some other difference, we performed siRNA knockdown experiments. Ly49Q expression in the Ly49Q^{hi} RAW264 cells was down-modulated by introducing Ly49Q antisense RNA, and the CpG-induced IL-6 production was examined. The expression of Ly49Q short hairpin RNA in the Ly49Q^{hi} RAW264 cells resulted in diminished IL-6 production in response to CpG (supplemental Figure 3A-B). The down-modulation of Ly49Q expression also caused a decrease in lysosome-like vesicular structures after CpG stimulation, implying a functional correlation between Ly49Q and lysosome and/or vesicle trafficking (supplemental Figure 3C). In addition, Ly49Q expression was induced in Ly49Q^{lo} RAW264 cells by IFN-γ treatment, as we reported previously (supplemental Figure 3D). In association with the increased Ly49Q expression, the IL-6 production and vacuolar formation by CpG stimulation were recovered in these originally Ly49Q^{lo} RAW cells (supplemental Figure 3E-F). Furthermore, the inhibition of Ly49Q expression using Ly49Q-specific short hairpin RNA in IFN-γ-treated RAW264 cells diminished the CpG-induced IL-6 production and vacuolar formation, indicating that Ly49Q is important for the IL-6 production triggered by TLR9 (supplemental Figure 3G-H). Therefore, TLR9-mediated cytokine production in RAW264 cells was also dependent on Ly49Q.

Defective TLR9 trafficking in the absence of Ly49Q

Therefore, we next investigated the intracellular trafficking of a TLR9-GFP fusion protein using the Ly49Q^{hi} and Ly49Q^{lo} RAW264 cells. Two hours after CpG stimulation, internalized CpG was colocalized with TLR9 in endosomes in both the Ly49Q^{hi} and Ly49Q^{lo} RAW264 cells (Figure 3D). However, there were great differences in the diameter, number, and cytoplasmic localizations of the CpG/TLR9 endosomes between the Ly49Q^{hi} and Ly49Q^{lo} RAW264 cells. In the Ly49Q^{lo} RAW264 cells, the diameters of the TLR9^{+} vesicles appeared smaller than in the Ly49Q^{hi} RAW264 cells (Figure 3D). In addition, several TLR9^{+} vesicles were observed scattered throughout the cytoplasm in the Ly49Q^{lo} RAW264 cells. After 24 hours of stimulation, the difference in TLR9 distribution between the Ly49Q^{lo} and Ly49Q^{hi} RAW264 cells was remarkable. TLR9 in the Ly49Q^{hi} RAW264 cells was localized along tubular endosomal structures and distributed at the edges of protrusions that were focal adhesion-like attachment sites. In contrast, in the Ly49Q^{lo} RAW264 cells, even though the TLR9^{+} vesicles colocalized with the CpG-containing endosomes, they remained scattered in the cytoplasm, and no vesicular fusion or elongation was observed. These tubular structures did not colocalize with either Rab11 or the transferrin receptor (data not shown).

Defects in tubular endolysosome extension, as observed in the Ly49Q knockout pDCs and macrophages, were also observed in Ly49Q^{lo} RAW264 cells (Figure 3E-F). Kinetic analyses of CpG trafficking demonstrated that both Ly49Q^{hi} and Ly49Q^{lo} RAW264 cells internalized CpG, although the amount of internalized CpG in Ly49Q^{lo} RAW264 cells seemed slightly lower than in Ly49Q^{hi} RAW264 cells at the early time point (1 hour; Figure 3E). After 8 hours of CpG stimulation, in the Ly49Q^{hi} RAW264 cells, CpG-containing endosomes appeared to spread or diffuse through the cytoplasm, in contrast to Ly49Q^{lo} RAW264 cells, which showed no diffuse distribution in CpG fluorescence in the cytoplasm. In addition, no obvious change of distribution pattern was observed in Ly49Q^{lo} RAW264 cells from 4 to 8 hours. A remarkable difference was also observed after 24 hours of CpG stimulation in the extension of tubular endolysosomal structures (Figure 3F). These results strongly suggest that the CpG trafficking in RAW264 cells was also regulated by Ly49Q.

Mitogen-activated protein kinase activation, but not NF-κB-related transcription factor expression, was affected by Ly49Q

Next, we examined which signaling pathways could be affected by Ly49Q. RT-PCR analyses revealed no great differences in the expression of NF-κB–related transcription factors between the Ly49Q^{hi} and Ly49Q^{lo} RAW264 cells (supplemental Figure 4; data not shown). However, the TLR9-triggered activation of p38 was severely impaired in the Ly49Q^{lo} RAW264 cells (Figure 4A). In addition, CpG-induced JNK activation was dysregulated in the Ly49Q^{lo} RAW264 cells. The activation of JNK in Ly49Q^{hi} RAW264 cells was sustained between 4 and 7 hours after CpG stimulation, but in the Ly49Q^{lo} RAW264 cells, the level of phospho-JNK decreased during this time (Figure 4B). In addition, immunohistochemical analyses clearly showed that Ly49Q colocalized with phosphorylated p38 in late endosome/lysosome compartments after CpG stimulation. A portion of the phosphorylated JNK also colocalized with LAMP-1^{+} late endosome compartments (Figure 4C). These results strongly suggest that Ly49Q influences TLR9-mediated p38 and JNK activation in the late endosome/lysosome compartments.

Ly49Q was internalized and recycled through an ITIM-mediated mechanism

To obtain insights into a mechanism of the Ly49Q-mediated TLR-containing vesicular trafficking, we analyzed trafficking of Ly49Q and its ligand, major histocompatibility complex (MHC) class I. We previously demonstrated that Ly49Q associates with MHC class I in *cis* at the cell surface.[20] By confocal microscopic analyses, we found that Ly49Q was colocalized with H-2K^{b} in peritoneal exudate macrophages (Figure 5A). This colocalization occurred not only at the cell surface, but also in cytoplasmic vesicles, suggesting that Ly49Q was internalized together with H-2K^{b}. We next tested whether the removal of β_2-microglobulin (β_2m) from the cell surface by acid treatment would elicit binding of the H-2K^{b} tetramer to Ly49Q, as shown for Ly49A.[13] As we previously reported, Ly49Q on the pDCs in C57BL/6 mice showed

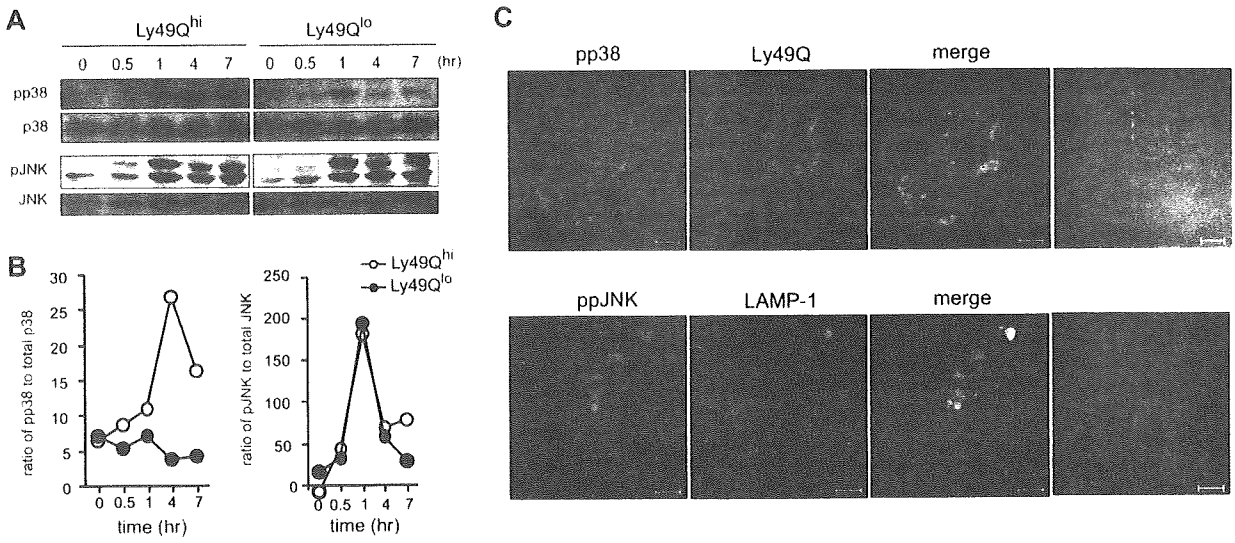

Figure 4. Ly49Q is involved in the regulation of MAP kinase activation after CpG stimulation. (A) Activation kinetics of p38 and JNK. RAW264 cells were treated with CpG (0.3 μM) for the indicated periods, and the total cell lysates were prepared by directly adding SDS sample buffer. The total lysates were separated by SDS–polyacrylamide gel electrophoresis, and the activation of p38 and JNK was examined by Western blotting. (B) The signal intensity (pixel numbers) of phosphorylated MAP kinases was normalized to that of each total MAP kinase, and semiquantitative values for the MAP kinase activation are shown. (C) Intracellular distribution of phosphorylated p38 and JNK in the presence of CpG stimulation. FLAG-tagged Ly49Q expression plasmids were introduced into Ly49Q^{hi} RAW264 cells, and 24 hours after transfection, the cells were incubated with unlabeled CpG (0.3 μM) for 2 hours. The cells were then fixed and stained with antibodies against FLAG and phosphorylated p38. To analyze the distribution of phosphorylated JNK, Ly49Q^{lo} RAW264 cells were treated with CpG for 2 hours and stained with antibodies against phospho-JNK and LAMP-1.

low levels of H-2K^b binding (Figure 5B).[20] C57BL/6 β_2m $^{-/-}$ pDCs showed increased H-2K^b binding, which was completely inhibited by an anti-Ly49Q antibody. These results indicate that Ly49Q associates with H-2K^b in a *cis* configuration. The acid treatment of pDCs did not affect the H-2K^b binding, even though β_2m was successfully removed from the cell surface (Figure 5C-D; data not shown). Furthermore, neither the cell viability nor the Ly49Q expression levels on the cell surface were affected by acid treatment (data not shown). These results strongly suggested that Ly49Q's association with H-2K^b is β_2m independent and stable under acidic conditions; therefore, this interaction should be sustained in intracellular acidic compartments, such as endosomes/lysosomes.

Next, we asked whether the ITIM of Ly49Q was involved in the internalization of Ly49Q, because the tyrosine motifs (Yxxϕ) in ITIMs have been suggested to function as an internalization signal.[21] We first investigated Ly49Q endocytosis in the presence of various inhibitors of membrane trafficking, using Ly49Q-null myeloid lineage WEHI3 cells transduced with Ly49Q-WT or an ITIM-less mutant (Ly49Q-YF). In the absence of inhibitors, Ly49Q-WT was largely observed at the cell surface, but Ly49Q-YF inhabited perinuclear intracellular granules (Figure 5E). Methyl-β-cyclodextrin, which inhibits raft-dependent endocytosis by depleting cholesterol from the plasma membrane,[22] abrogated both the perinuclear distribution of Ly49Q-YF and the juxtamembranous endosomal distribution of Ly49Q-WT. Chlorpromazine, an inhibitor of clathrin-dependent endocytosis,[23] did not inhibit the internalization of either Ly49Q-YF or Ly49-WT. These results strongly suggest that Ly49Q is internalized via lipid raft-mediated endocytosis, and that the ITIM is not necessary for endocytosis itself, but important for the retention of Ly49Q at the cell surface.

We also found that the internalized endosomes were transported along microtubules, because nocodazole treatment strikingly diminished the accumulation of Ly49Q-YF in the perinuclear regions.[24] Importantly, treatment with a phosphatase inhibitor, sodium vanadate,[25] caused Ly49Q-WT to be redistributed to the perinuclear region in the same pattern as Ly49Q-YF. Given that Ly49Q-WT can associate with tyrosine phosphatases via its ITIM, these results suggest that the ITIM-associated phosphatase is important for regulating the intracellular distribution of Ly49Q. Because MHC class I recycles between the cell surface and endosomes, this finding also suggests that Ly49Q recycles together with MHC class I along microtubules in the steady state.

Discussion

In this study, we demonstrated that an inhibitory receptor, Ly49Q, plays an important role in the signaling of TLR9 by controlling the intracellular trafficking of TLR9 and CpG. The spatiotemporal regulation of the vesicular compartments containing TLR9 and CpG and their associated adaptor proteins is crucial for TLR9 signaling.[5,6] Ly49Q itself was internalized and appeared to move along microtubules in the steady state. The observation that Ly49Q associated with MHC class I in a *cis* configuration, even in an acidic environment, strongly suggests that Ly49Q recycles together with MHC class I. Importantly, the Ly49Q movement was regulated by an ITIM- and tyrosine phosphatase-dependent mechanism. Because Ly49Q itself can recruit tyrosine phosphatases such as SHP-1 and SHP-2 to the ITIM,[7] it is possible that Ly49Q-associated phosphatases play a role in the trafficking of Ly49Q itself.

How Ly49Q influences TLR9/CpG trafficking in addition to its own recycling process is an important question. Not all the CpG-containing endosomes included Ly49Q, and some endosomes contained only Ly49Q. This observation suggests that Ly49Q-containing and CpG-containing endosomes fused after these molecules were internalized separately. In endosomes/lysosomes, where the pH ranges from 5.0 to 6.5 depending on the type of compartment, some receptor-ligand interactions are disrupted due to the acidic environment. However, internalized Ly49Q might maintain an association with MHC class I in

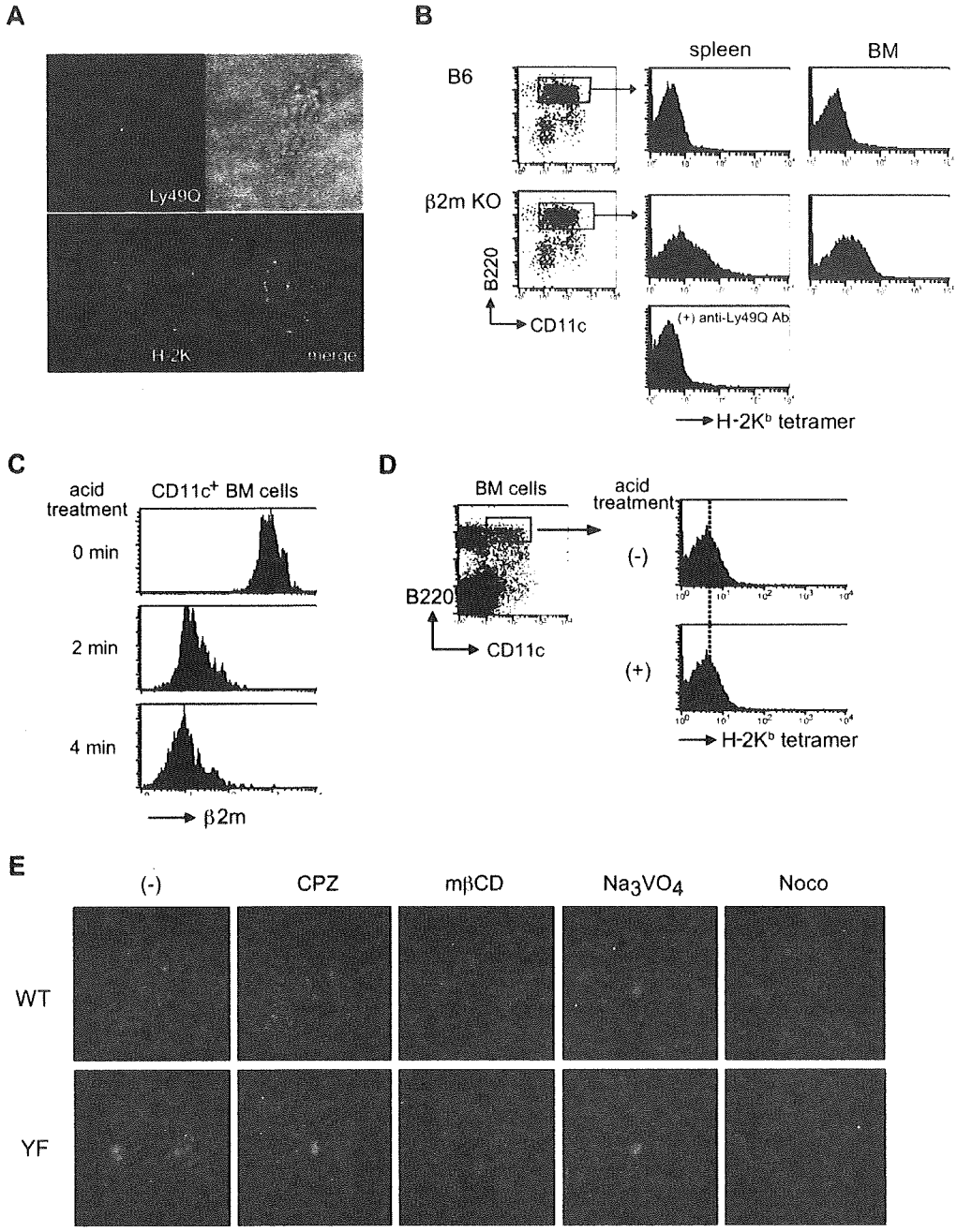

Figure 5. Ly49Q was internalized with MHC class I, and its localization was regulated in an ITIM- and tyrosine phosphatase-dependent manner. (A) Colocalization of Ly49Q with H-2K^b in intracellular vesicular compartments. Peritoneal exudation macrophages were prepared from Ly49Q Tg mice and examined for Ly49Q (red) and MHC class I (green) by immunohistochemical analyses with a confocal microscope. FLAG-tagged Ly49Q in Tg mice was detected with an anti-FLAG antibody. (B) Binding of H-2K^b tetramer to pDCs. Cells enriched in bone marrow pDCs were obtained by AutoMACS using an anti–plasmacyloid DC Ag-1 antibody, and the binding of PE-conjugated H-2K^b tetramer was examined by flow cytometry. In the absence of β_2m, binding of the H-2K^b tetramer in *trans* was detectable due to loss of the *cis* interaction. The tetramer binding was abrogated by an anti-Ly49Q antibody. (C) Removal of β_2m from the cell surface by acid treatment. Bone marrow cells were treated with citrate buffer (0.133 M citric acid and 0.066 M Na_2HPO_4, pH 3.3) at 20°C for the indicated periods. Removal of β_2m from the cell surface was confirmed by a decreased fluorescence intensity of anti-β_2m antibody staining. CD11c$^+$ cells were gated and analyzed. (D) Binding of H-2K^b tetramer before and after acid treatment. H-2K^b tetramer bound in *trans* to Ly49Q after the removal of β_2m from the cell surface, indicating that the *cis* interaction between Ly49Q and H-2K^b was still maintained, and the interaction was β_2m independent and acid resistant. (E) ITIM and tyrosine phosphatase dependence of Ly49Q redistribution. WEHI3 transfectants expressing Ly49Q-WT or Ly49Q-YF were incubated at 37°C in the presence or absence of the indicated inhibitors of membrane trafficking. The cells were then fixed and stained with an anti-FLAG antibody to visualize Ly49Q.

endosomes, because the Ly49Q-MHC class I association was β_2m independent and acid resistant. In fact, Ly49Q and MHC class I were still colocalized in the endosomes/lysosomes after being internalized. Therefore, Ly49Q may influence endosome behavior and TLR9 signaling events in such vesicular compartments through an interaction with MHC class I, which may contribute to the sustained activation of mitogen-activated protein (MAP) kinases that are colocalized with Ly49Q at the endosomes. Further investigations focusing on the roles of this inhibitory receptor not only at the plasma membrane, but also at

intracellular vesicular compartments, may help us in understanding the fine-tuning of immune responses.

In this study, we found that the TLR9-triggered extension of tubular endolysosome structures was severely impaired in both Ly49Q^{lo} RAW264 cells and Ly49Q knockout pDC's and macrophages. Tubular endolysosomal structures have attracted attention for their functional associations not only with TLR signaling, but also with various cellular activities, including cytokine secretion and phagocytosis, and antigen presentation.[3,18,26-30] Although neither the regulatory mechanisms that govern the formation and trafficking of these compartments nor their nature are fully understood, it has been established that the dynamic movement and reconstitution of the TLR9-associated endoplasmic reticulum and endolysosomes provide a site where TLR9-associated signal complexes containing the receptor, the ligand, MyD88, and IFN regulatory factor 7 can be assembled.[3,5] In addition, the location and retention of these molecules in endosomes are the key factors controlling the nature of TLR9 responses. These observations together lead to a novel concept that the trafficking of TLR signaling complexes to the correct membrane compartment with appropriate timing may be important for eliciting effective and controlled immune responses. In light of our present findings, we propose that Ly49Q is involved in the optimization of TLR9 signaling by controlling the redistribution of endolysosome compartments spatiotemporally.

In addition to the impaired formation of tubular endolysosomal structures, Ly49Q^{lo} RAW264 cells contained smaller TLR9/CpG endosomes than Ly49Q^{hi} cells. This observation suggests that Ly49Q plays a role not only in the intracellular movement of endosomes/lysosomes, but also in the endocytic process itself. Given that the CpG-containing endosomes were smaller in Ly49Q^{lo} than in Ly49Q^{hi} RAW264 cells, Ly49Q may affect the dimension of the endocytic cups. It has been proposed that the Yxxϕ (where ϕ is a hydrophobic amino acid) of the ITIM sequence functions as the internalization signal for membrane protein trafficking.[31] Tyrosine-mediated internalization has been demonstrated for inhibitory receptors such as cytotoxic T lymphocyte-associated antigen-1 and CD33.[31,32] In these receptors, tyrosine phosphorylation of the ITIM is essential for the recruitment of the internalization machinery, including the μ2 or suppressor of cytokine signaling 3-E3 ligase complex, and the subsequent internalization and degradation of the receptors. However, Ly49Q internalization seems to be mediated by a different mechanism from that reported for cytotoxic T lymphocyte-associated antigen-1 and CD33, because the ITIM is essential for the maintenance of Ly49Q at the cell surface, and Ly49Q-YF, whose mutant ITIM lacked tyrosine, was internalized. Alternatively, Ly49Q may be involved in the directional transport of recycling endosomes from the perinuclear region to the plasma membrane along microtubules. The accumulation of Ly49Q-YF at the perinuclear region may reflect stagnating endolysosomes that ought to have been added to the tubular endolysosomal structures to extend them. Importantly, the improper trafficking of TLR9/CpG vesicular compartments in Ly49Q$^-$ and Ly49Q^{lo} cells was closely related to the impaired production of cytokines such as IFN-β and IL-6. Although the precise molecular basis for Ly49Q's regulation of endosome/lysosome trafficking is still largely unknown, our data indicate that Ly49Q is important for the physical positioning of TLR9 signaling within a cell.

The mechanistic linkages among the tubular endolysosome extension, MAP kinase activation, and cytokine production still need to be elucidated. We showed that p38 activation was impaired, and JNK activation was temporally dysregulated in Ly49Q^{lo} cells during CpG stimulation. We also demonstrated that phospho-p38 and phospho-JNK distributed to Ly49Q-containing endosome/lysosome compartments. Therefore, TLR9, CpG, pp38, pJNK, and Ly49Q might be colocalized in the same endosomes/lysosomes and functionally associated. The JNK pathway is required for the formation of the immunologic synapse between NK and their target cells: the expression of dominant-negative JNK or its siRNA knockdown blocks the cytotoxic granule movement along microtubules to the interface between the NK and its target cells, preventing NK cell polarization.[33] The cytotoxic granules have been suggested to share a common biogenesis with lysosomes.[34] Therefore, it is possible that an impairment of sustained JNK activation disrupts the directional movement of TLR9/CpG-riding endolysosomes along microtubules. In addition to JNK, p38 modulates endocytosis, by regulating a guanosine diphosphate dissociation inhibitor in the cytosolic cycle of Rab5, a key regulator of endocytic membrane traffic.[35,36] Further detailed analyses will be necessary to examine these possibilities.

Our present study established that Ly49Q is important for the regulation of TLR trafficking, which is associated with temporally regulated MAP kinase activation and cytokine production. The inappropriate positioning and timing of TLR9 signaling complexes may be caused by the lack of Ly49Q, resulting in impaired cytokine responses. Therefore, the fine-tuning of the intracellular trafficking of TLR9/CpG compartments by such an inhibitory receptor might be crucial for optimizing the responses to various infectious microbes. It is intriguing that the inflammatory cell-specific inhibitory receptor, Ly49Q, is a key regulator for the correct positioning of the TLR9 signaling complex. Understanding the multiple functions of this inhibitory receptor will help reveal the molecular bases of TLR9 receptor functioning as well as that of the NK receptors, and will shed light on the origin and role of inhibitory receptors recognizing MHC class I in the regulation of immune cells ranging from macrophages to NK cells.

Acknowledgments

We thank Dr T. Kitamura for providing the pMxs-IRES-GFP plasmid; Dr K. Miyake for the TLR9-GFP expression plasmid; Drs C. R. Roy and A. Hubber for the Rab5-DsRed expression plasmid; Dr Takayanagi for the Ly49Q knockdown plasmids; Drs L. A. Miglietta and G. E. Gray for critical reading of this manuscript; Drs T. Okamura and M. Goto, S. Takahashi, and other members of Sankyo Lab Inc of Japan for animal care; and M. Nakasuji for technical support. We also thank Drs H. Sorimachi and K. Nishikawa and the staff of our laboratory for helpful discussion.

This work was supported by grants-in-aid for scientific research from the Ministry of Education, Science, Sports, and Culture of Japan (17590445 and 19590507 to N.T.-S.; 1839012 to K.I.), and grants from the Ministry of Health and Welfare and the Naito Memorial Foundation.

Authorship

Contribution: M.Y., A.T., E.K., S.S., and K.I. performed experiments; T.D., K.I., T.S., and A.P.M. analyzed results; and N.T.-S. designed the research and wrote the paper.

Conflict-of-interest disclosure: The authors declare no competing financial interests.

Correspondence: Noriko Toyama-Sorimachi, Department of Gastroenterology, Research Institute, International Medical Center of Japan, Toyama 1-21-1, Shinjuku-ku, Tokyo 162-8655, Japan; e-mail: nsorima@ri.imcj.go.jp.

References

1 Kawai T, Akira S. TLR signaling. *Semin Immunol* 2007;19:24-32.

2 Barton GM, Kagan JC, Medzhitov R. Intracellular localization of Toll-like receptor 9 prevents recognition of self DNA but facilitates access to viral DNA. *Nat Immunol*. 2006;7:49-56.

3 Latz E, Schoenemeyer A, Visintin A, et al. TLR9 signals after translocating from the ER to CpG DNA in the lysosome. *Nat Immunol*. 2004;5:190-198.

4 Kim YM, Brinkmann MM, Paquet ME, Ploegh HL. UNC93B1 delivers nucleotide-sensing Toll-like receptors to endolysosomes. *Nature*. 2008;452:234-238.

5 Honda K, Ohba Y, Yanai H, et al. Spatiotemporal regulation of MyD88-IRF-7 signalling for robust type-I interferon induction. *Nature*. 2005;434:1035-1040.

6 Guiducci C, Ott G, Chan JH, et al. Properties regulating the nature of the plasmacytoid dendritic cell response to Toll-like receptor 9 activation. *J Exp Med*. 2006;203:1999-2008.

7 Toyama-Sorimachi N, Tsujimura Y, Maruya M, et al. Ly49Q, a member of the Ly49 family that is selectively expressed on myeloid lineage cells and involved in regulation of cytoskeletal architecture. *Proc Natl Acad Sci U S A*. 2004;101:1016-1021.

8 Makrigiannis AP, Pau AT, Schwartzberg PL, McVicar DW, Beck TW, Anderson SK. A BAC contig map of the Ly49 gene cluster in 129 mice reveals extensive differences in gene content relative to C57BL/6 mice. *Genomics*. 2002;79:437-444.

9 Toyama-Sorimachi N, Omatsu Y, Onoda A, et al. Inhibitory NK receptor Ly49Q is expressed on subsets of dendritic cells in a cellular maturation- and cytokine stimulation-dependent manner. *J Immunol*. 2005;174:4621-4629.

10 Omatsu Y, Iyoda T, Kimura Y, et al. Development of murine plasmacytoid dendritic cells defined by increased expression of an inhibitory NK receptor, Ly49Q. *J Immunol*. 2005;174:6657-6662.

11 Kamogawa-Schifter Y, Ohkawa J, Namiki S, Arai N, Arai K, Liu Y. Ly49Q defines 2 pDC subsets in mice. *Blood*. 2005;105:2787-2792.

12 Tai LH, Goulet ML, Belanger S, et al. Positive regulation of plasmacytoid dendritic cell function via Ly49Q recognition of class I MHC. *J Exp Med*. 2008;205:3187-3199.

13 Doucey MA, Scarpellino L, Zimmer J, et al. Cis association of Ly49A with MHC class I restricts natural killer cell inhibition. *Nat Immunol*. 2004;5:328-336.

14 Tanimura N, Saitoh S, Matsumoto F, Akashi-Takamura S, Miyake K. Roles for LPS-dependent interaction and relocation of TLR4 and TRAM in TRIF-signaling. *Biochem Biophys Res Commun*. 2008;368:94-99.

15 Matsumoto F, Saitoh S, Fukui R, et al. Cathepsins are required for Toll-like receptor 9 responses. *Biochem Biophys Res Commun*. 2008;367:693-699.

16 Datta SK, Redecke V, Prilliman KR, et al. A subset of Toll-like receptor ligands induces cross-presentation by bone marrow-derived dendritic cells. *J Immunol*. 2003;170:4102-4110.

17 Rutz M, Metzger J, Gellert T, et al. Toll-like receptor 9 binds single-stranded CpG-DNA in a sequence- and pH-dependent manner. *Eur J Immunol*. 2004;34:2541-2550.

18 Vyas JM, Kim YM, Artavanis-Tsakonas K, Love JC, Van der Veen AG, Ploegh HL. Tubulation of class II MHC compartments is microtubule dependent and involves multiple endolysosomal membrane proteins in primary dendritic cells. *J Immunol*. 2007;178:7199-7210.

19 Wehland J, Weber K. Turnover of the carboxy-terminal tyrosine of α-tubulin and means of reaching elevated levels of detyrosination in living cells. *J Cell Sci*. 1987;88:185-203.

20 Tai LH, Goulet ML, Belanger S, et al. Recognition of H-2K^b by Ly49Q suggests a role for class Ia MHC regulation of plasmacytoid dendritic cell function. *Mol Immunol*. 2007;44:2638-2646.

21 Boll W, Ohno H, Songyang Z, et al. Sequence requirements for the recognition of tyrosine-based endocytic signals by clathrin AP-2 complexes. *EMBO J*. 1996;15:5789-5795.

22 Keller P, Simons K. Cholesterol is required for surface transport of influenza virus hemagglutinin. *J Cell Biol*. 1998;140:1357-1367.

23 Wang LH, Rothberg KG, Anderson RG. Mis-assembly of clathrin lattices on endosomes reveals a regulatory switch for coated pit formation. *J Cell Biol*. 1993;123:1107-1117.

24 Mukhopadhyay A, Funato K, Stahl PD. Rab7 regulates transport from early to late endocytic compartments in *Xenopus* oocytes. *J Biol Chem*. 1997;272:13055-13059.

25 Courtneidge SA. Activation of the pp60c-*src* kinase by middle T antigen binding or by dephosphorylation. *EMBO J*. 1985;4:1471-1477.

26 Woodman PG, Futter CE. Multivesicular bodies: co-ordinated progression to maturity. *Curr Opin Cell Biol*. 2008;20:408-414.

27 Harrison RE, Bucci C, Vieira OV, Schroer TA, Grinstein S. Phagosomes fuse with late endosomes and/or lysosomes by extension of membrane protrusions along microtubules: role of Rab7 and RILP. *Mol Cell Biol*. 2003;23:6494-6506.

28 Racoosin EL, Swanson JA. Macropinosome maturation and fusion with tubular lysosomes in macrophages. *J Cell Biol*. 1993;121:1011-1020.

29 Hollenbeck PJ, Swanson JA. Radial extension of macrophage tubular lysosomes supported by kinesin. *Nature*. 1990;346:864-866.

30 Heuser J. Changes in lysosome shape and distribution correlated with changes in cytoplasmic pH. *J Cell Biol*. 1989;108:855-864.

31 Shiratori T, Miyatake S, Ohno H, et al. Tyrosine phosphorylation controls internalization of CTLA-4 by regulating its interaction with clathrin-associated adaptor complex AP-2. *Immunity*. 1997;6:583-589.

32 Orr SJ, Morgan NM, Elliott J, et al. CD33 responses are blocked by SOCS3 through accelerated proteasomal-mediated turnover. *Blood*. 2007;109:1061-1068.

33 Li C, Ge B, Nicotra M, et al. JNK MAP kinase activation is required for MTOC and granule polarization in NKG2D-mediated NK cell cytotoxicity. *Proc Natl Acad Sci U S A*. 2008;105:3017-3022.

34 Clark R, Griffiths GM. Lytic granules, secretory lysosomes and disease. *Curr Opin Immunol*. 2003;15:516-521.

35 Cavalli V, Vilbois F, Corti M, et al. The stress-induced MAP kinase p38 regulates endocytic trafficking via the GDI:Rab5 complex. *Mol Cell*. 2001;7:421-432.

36 Mace G, Miaczynska M, Zerial M, Nebreda AR. Phosphorylation of EEA1 by p38 MAP kinase regulates μ opioid receptor endocytosis. *EMBO J*. 2005;24:3235-3246.

Biochemical and Biophysical Research Communications 393 (2010) 432–438

Contents lists available at ScienceDirect

Biochemical and Biophysical Research Communications

journal homepage: www.elsevier.com/locate/ybbrc

Ly49Q, an ITIM-bearing NK receptor, positively regulates osteoclast differentiation

Mikihito Hayashi [a,c], Tomoki Nakashima [a,b,c], Tatsuhiko Kodama [d], Andrew P. Makrigiannis [e], Noriko Toyama-Sorimachi [f], Hiroshi Takayanagi [a,b,c,*]

[a] Department of Cell Signaling, Graduate School of Medical and Dental Science, Tokyo Medical and Dental University, Yushima 1-5-45, Bunkyo-ku, Tokyo 113-8549, Japan
[b] Japan Science and Technology Agency, ERATO, Takayanagi Osteonetwork Project, Yushima 1-5-45, Bunkyo-ku, Tokyo 113-8549, Japan
[c] Global Center of Excellence Program, International Research Center for Molecular Science in Tooth and Bone Diseases, Yushima 1-5-45, Bunkyo-ku, Tokyo 113-8549, Japan
[d] Research Center for Advanced Science and Technology, Department of Molecular Biology and Medicine, University of Tokyo, Tokyo 153-8904, Japan
[e] Laboratory of Molecular Immunology, Institute de Recherches Cliniques de Montreal, Montreal, Quebec, Canada H2W 1R7
[f] Department of Gastroenterology, Research Institute, International Medical Center of Japan, Toyama 1-21-1, Shinjuku-ku, Tokyo 162-8655, Japan

ARTICLE INFO

Article history:
Received 29 January 2010
Available online 12 February 2010

Keywords:
Ly49Q
Osteoclast
Osteoimmunology
ITIM

ABSTRACT

Osteoclasts, multinucleated cells that resorb bone, play a key role in bone remodeling. Although immunoreceptor tyrosine-based activation motif (ITAM)-mediated signaling is critical for osteoclast differentiation, the significance of immunoreceptor tyrosine-based inhibitory motif (ITIM) has not been well understood. Here we report the function of Ly49Q, an Ly49 family member possessing an ITIM motif, in osteoclastogenesis. Ly49Q is selectively induced by receptor activator of nuclear factor-κB (NF-κB) ligand (RANKL) stimulation in bone marrow-derived monocyte/macrophage precursor cells (BMMs) among the Ly49 family of NK receptors. The knockdown of Ly49Q resulted in a significant reduction in the RANKL-induced formation of tartrate-resistance acid phosphatase (TRAP)-positive multinucleated cells, accompanied by a decreased expression of osteoclast-specific genes such as *Nfatc1*, *Tm7sf4*, *Oscar*, *Ctsk*, and *Acp5*. Osteoclastogenesis was also significantly impaired in Ly49Q-deficient cells *in vitro*. The inhibitory effect of Ly49Q-deficiency may be explained by the finding that Ly49Q competed for the association of Src-homology domain-2 phosphatase-1 (SHP-1) with paired immunoglobulin-like receptor-B (PIR-B), an ITIM-bearing receptor which negatively regulates osteoclast differentiation. Unexpectedly, Ly49Q deficiency did not lead to impaired osteoclast formation *in vivo*, suggesting the existence of a compensatory mechanism. This study provides an example in which an ITIM-bearing receptor functions as a positive regulator of osteoclast differentiation.

Introduction

Bone homeostasis is controlled by the coordinated balance maintained between bone formation by osteoblasts and bone resorption by osteoclasts [1]. Osteoclasts, multinucleated cells that uniquely have the ability to resorb bone, play a central role in calcium homeostasis as well as bone remodeling [2]. Increased osteoclast differentiation and function have been implicated in the pathogenesis of various osteopenic conditions, including postmenopausal osteoporosis and bone loss in inflammatory arthritis [3,4]. Therefore, understanding the regulatory mechanisms of osteoclast differentiation and function is important for the development of novel therapeutic strategies for these disorders.

Osteoclasts differentiate from monocyte/macrophage lineage cells in the presence of macrophage-colony stimulating factor (M-CSF) and receptor activator of nuclear factor-κB (NF-κB) ligand (RANKL) [1,2]. This process is tightly regulated by mesenchymal lineage cells such as osteoblasts and bone marrow stromal cells, which provide M-CSF and RANKL [1,2]. M-CSF signaling through its receptor, c-Fms, is required for the survival and proliferation of osteoclast precursor cells [5]. RANKL binding to its receptor, RANK, results in the activation of tumor necrosis factor receptor-associated factor 6 (TRAF6), c-Fos, and calcium signaling pathways, each of which is essential for the induction and activation of nuclear factor of activated T cells (NFAT) c1, a critical transcription factor for osteoclastogenesis [1,6]. In fact, mice deficient in RANKL, RANK, TRAF6, c-Fos, and NFATc1 exhibit severe osteopetrosis due to impaired osteoclastogenesis [1,3,7].

In addition to RANKL and M-CSF, costimulatory signals mediated by immunoreceptor tyrosine-based activation motif (ITAM)-bearing adaptors, DNAX-activating protein 12 (DAP12), and Fc

* Corresponding author. Address: Department of Cell Signaling, Graduate School of Medical and Dental Sciences, Tokyo Medical and Dental University, Yushima 1-5-45, Bunkyo-ku, Tokyo 113-8549, Japan. Fax: +81 3 5803 0192.
E-mail address: taka.csi@tmd.ac.jp (H. Takayanagi).

0006-291X/$ - see front matter © 2010 Elsevier Inc. All rights reserved.
doi:10.1016/j.bbrc.2010.02.013

receptor common γ subunit (FcRγ), are indispensable for osteoclastogenesis [8,9]. The immunoglobulin-like receptors, such as triggering receptors expressed on myeloid cells-2 (TREM-2), paired immunoglobulin-like receptor (PIR)-A, osteoclast-associated receptor (OSCAR), and signal-regulatory protein (SIRP) β1, which associate with DAP12 or FcRγ in osteoclast precursor cells, play a key role in the costimulatory signals required for osteoclastogenesis [1,10], although the ligands of these receptors in the skeletal system have not yet been identified.

In the immune system, the balance between the activating signals mediated by the ITAM and the inhibitory signals mediated by the immunoreceptor tyrosine-based inhibitory motif (ITIM) determine the level of the immune response [11,12]. The activating signals are mediated by the tyrosine kinases, including the Src and spleen tyrosine kinase (Syk) families, whereas the inhibitory signals are mediated by protein tyrosine phosphatases and lipid phosphatases which are recruited to ITIM [12]. Interestingly, viable motheaten mice (me^v/me^v), which have a catalytically defective Src-homology domain-2 phosphatase-1 (SHP-1), exhibit severe osteoporosis caused by enhanced osteoclastic bone resorption, suggesting that SHP-1 controls osteoclast differentiation and function [13,14]. Although recent studies have reported that certain ITIM-bearing receptors, including PIR-B, SIRPα, platelet endothelial cell adhesion molecule-1 (PECAM-1) and CMRF-35-like molecule-1 (CLM-1), inhibit osteoclastogenesis through SHP-1 activation [15–18], the function of the ITIM-bearing receptors remains to be elucidated further.

The murine Ly49 receptor family is comprised of both activating and inhibitory molecules in target cell recognition by natural killer (NK) cells [19]. Ly49Q is a type II transmembrane protein which contains the ITIM motif at the N-terminus of the cytoplasmic region and associates with MHC class I *in cis* [20]. Whereas most of the Ly49 receptors are expressed on NK cells, Ly49Q is expressed on plasmacytoid dendritic cells (pDCs), macrophages, and neutrophils, but not NK cells [20–22]. Several Ly49 receptors inhibit NK cell functions, including cytokine production and cytolytic activity. Treatment of activated macrophages with an anti-Ly49Q antibody induces rapid spreading and the formation of cell polarity through the reorganization of the actin cytoskeleton [20]. Following inhibitory Ly49 receptor engagement with MHC class I ligand, the phosphorylation of a tyrosine residue within the ITIM present in the cytoplasmic region facilitates the binding and activation of the SHP-1 and SHP-2 phosphatases, and the attenuation of intracellular signals [23]. Although Ly49Q is able to associate with SHP-1 and SHP-2 via its tyrosine-phosphorylated ITIM [20], toll-like receptor 9 (TLR9)-dependent antiviral responses were diminished *in vivo*, and the production of cytokines such as interferon-α (IFN-α) and interleukin (IL)-12 from pDCs in response to TLR9 was impaired *in vitro*, suggesting that Ly49Q is necessary for the activation of the innate immune response [24]. Similarly, the TLR9-mediated production of inflammatory cytokines such as IL-6 and tumor necrosis factor-α (TNF-α) was impaired in macrophages derived from Ly49Q-deficient mice [22].

In this study, we report that RANKL stimulation caused a selective induction of Ly49Q during osteoclast differentiation, which effect was diminished by FK506-mediated inhibition of calcineurin-NFAT activation. The knockdown or genetic ablation of Ly49Q in osteoclast precursor cells resulted in the significant suppression of osteoclastogenesis *in vitro*. Thus, these findings suggest that Ly49Q positively regulates osteoclast differentiation, and led us to investigate the mechanisms underlying this positive regulation and the bone phenotype in Ly49Q-deficient mice.

Materials and methods

Mice and analysis of the bone phenotype. The generation of Ly49Q-deficient mice was described previously [24]. All mice were maintained under specific-pathogen free conditions. Ly49Q-deficient mice were maintained and bred in the International Medical Center of Japan. All animal experiments were approved by the Animal Study Committee of Tokyo Medical and Dental University or the International Medical Center of Japan. Three-dimensional microcomputed tomography (microCT) scanning was performed using a ScanXmate-A100S Scanner (Comscan Techno, Kanagawa, Japan). Three-dimensional microCT images were reconstructed and the structural indices calculated using a three-dimensional image analysis system (TRI/3D-BON; RATOC System Engineering, Tokyo, Japan). Analyses of bone histology were performed as described [8,25,26].

In vitro osteoclastogenesis. *In vitro* osteoclastogenesis was performed as described previously [6,8,25,26]. Briefly, bone marrow cells were cultured with 10 ng/ml M-CSF (R&D Systems, Minneapolis, MN) to obtain bone marrow-derived monocyte/macrophage precursor cells (BMMs). These cells were cultured with 5 or 50 ng/ml RANKL (PeproTech, Rocky Hill, NJ) and M-CSF for 3 days. Osteoclastogenesis was evaluated by tartrate-resistance acid phosphatase (TRAP) staining.

Quantitative RT-PCR and GeneChip analysis. Real-time quantitative RT-PCR analysis was performed as described [26]. Briefly, total RNA was extracted by ISOGEN (NIPPON GENE, Tokyo, Japan) according to the manufacturer's instructions. First-strand cDNAs were synthesized from 0.5 μg of total RNA using Superscript III reverse transcriptase (Invitrogen, Carlsbad, CA). Quantitative RT-PCR analysis was performed with the LightCycler apparatus (Roche Applied Science, Indianapolis, IN) using SYBR Green Real time PCR Master Mix (TOYOBO, Osaka, Japan). All primer sequences are available upon request. GeneChip analysis was performed as described previously [6,27].

Flow cytometric analysis. BMMs were removed from culture plates by treatment with Trypsin–EDTA (Invitrogen). Cell surface expression of Ly49Q was confirmed by staining with biotinylated anti-Ly49Q antibody [20] followed by Streptavidin–allophycocyanin conjugates (eBioscience, San Diego, CA). Stained cells were analyzed by FACSCantoII using Diva software (BD Biosciences, San Jose, CA).

Knockdown analysis. The short hairpin RNA (shRNA) duplexes were constructed based on the sequences obtained from the shRNA library of the RNAi Consortium. RNA targeting regions with a hairpin sequence (shLy49Q-1 sense: 5′-gatccGTAAACAGATATGTGA GCATTCTCGAGAATGCTCACATATCTGTTTACTTTTTg-3′; shLy49Q-1 antisense: 5′- aattcAAAAAGTAAACAGATATGTGAGCATTCTCGAGAA TGCTCACATATCTGTTTACg-3′; shLy49Q-2 sense: 5′-gatccGAACA TGTCTACCCATGTATTCTCGAGAATACATGGGTAGACATGTTCTTTTTg-3′; shLy49Q-2 antisense: 5′-aattcAAAAAGAACATGTCTACC CATGTATTCTCGAGAATACATGGGTAGACATGTTCg-3′; shNFATc1 sense: 5′-gatccGCCGCAGAACACTACAGT TATCTCGAGATAACTG-TAGTGTTCTGCGGCTTTTTg-3′; shNFATc1 antisense: 5′- aatt-cAAAAAGCCGCAGAACACTACAGTTATCTCGAGATAACTGTAGTGTTC TGCGGCg-3′) were ligated into the RNAi-Ready pSIREN-RetroQ-ZsGreen Vector (Clontech, Mountain View, CA) at the BamHI and EcoRI sites. pSIREN-RetroQ-ZsGreen-shLy49Qs, pSIREN-RetroQ-ZsGreen-shNFATc1 or a control pSIREN-RetroQ-ZsGreen-shRNA that specifically targets Luciferase was used to transfect BMMs. The retrovirus supernatants were obtained by transfecting the retroviral vectors into the Plat-E packaging cell line using Fugene6 (Roche Applied Science). BMMs were infected with retroviruses for 12 h before RANKL stimulation.

Immunoblot analysis. Cell lysates were subjected to immunoblot analysis using specific antibodies for NFATc1 (Santa Cruz Biotechnology, Santa Cruz, CA), c-Fos (Calbiochem, La Jolla, CA), and β-actin (Sigma–Aldrich, St. Louis, MO). For immunoprecipitation analysis, cells were solubilized in lysis buffer (1% Nonidet P-40 in 50 mM NaCl, 50 mM Tris–HCl, 5 mM EDTA, 1 mM NaF, 2 mM

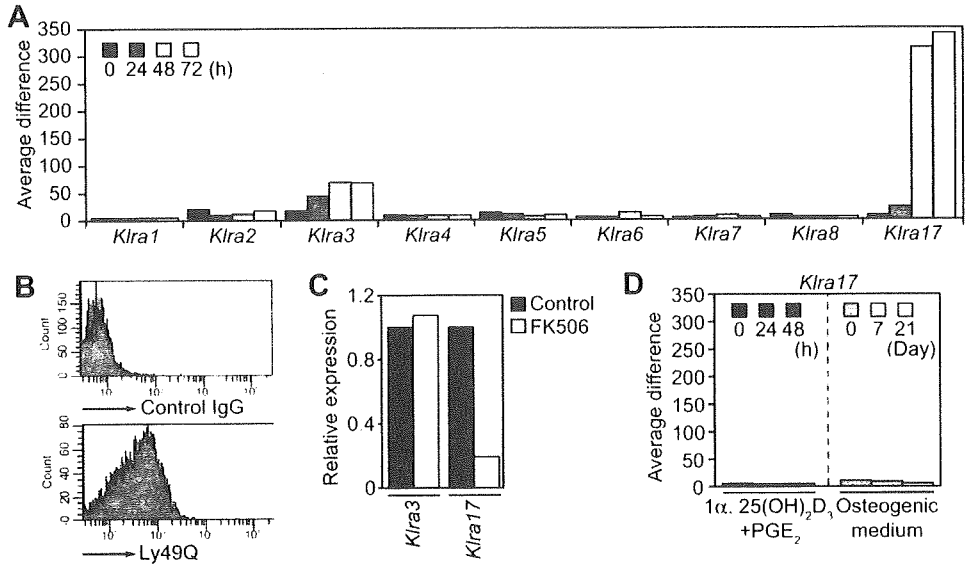

Fig. 1. Expression of Ly49 receptors in osteoclasts and osteoblasts. (A) GeneChip analysis of the mRNA expression of Ly49 receptors during osteoclast differentiation after RANKL stimulation. (B) Flow cytometric analysis of Ly49Q expression on BMMs treated with RANKL for 2 days. (C) Effect of FK506 treatment on the mRNA expression of *Klra3* and *Klra17* in osteoclasts. (D) GeneChip analysis of the mRNA expression of *Klra17* in calvarial osteoblasts treated with 10 nM 1α, 25(OH)$_2$D$_3$ and 1 μM PGE$_2$ or osteogenic medium (50 μM ascorbic acid, 10 nM dexamethasone and 10 mM β-glycerophosphate).

PMSF), supplemented with Complete Protease Inhibitor Cocktail (Roche Applied Science). Immunoprecipitation was carried out by incubation with the anti-SHP-1 antibody (Cell Signaling Technology, Beverly, MA) followed by the addition of protein G–Sepharose (GE Healthcare, Buckinghamshire, UK). Immune complexes were separated by electrophoresis followed by blotting with anti-PIR-B (R&D Systems), anti-PECAM-1(Santa Cruz Biotechnology), and anti-SHP-1 antibodies.

Statistical analysis. Statistical analysis was performed using the unpaired two-tailed Student's *t* test (*$P < 0.05$; **$P < 0.01$;

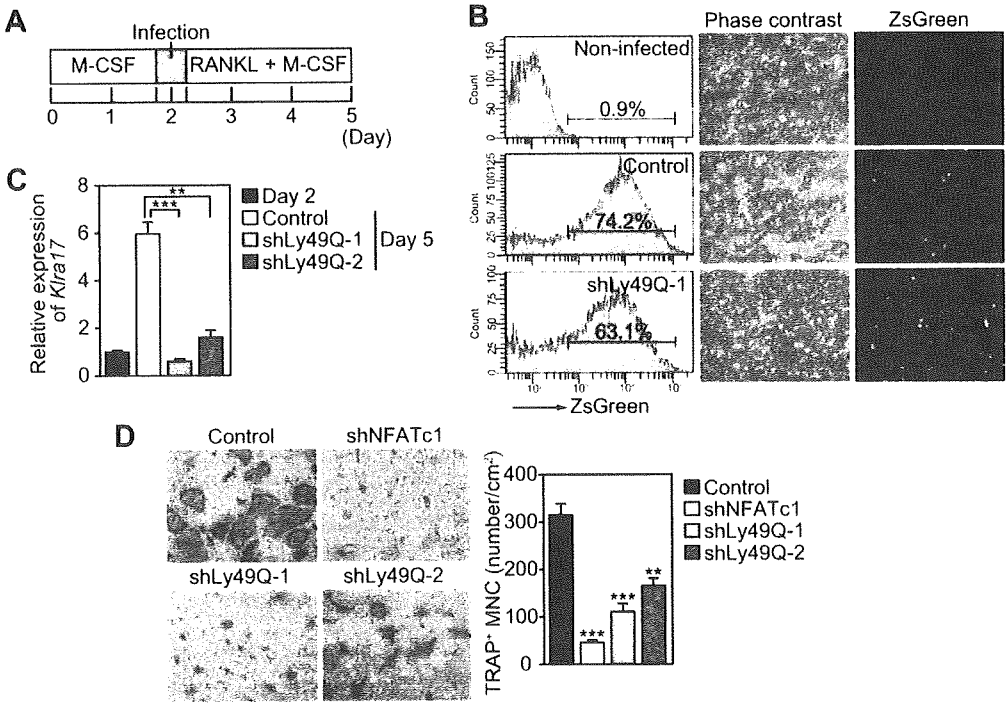

Fig. 2. Contribution of Ly49Q to RANKL-induced osteoclastogenesis. (A) A schematic of the *in vitro* osteoclast culture system and the retroviral transfer. The infected cells were cultured for 3 days in the presence of RANKL and M-CSF. (B) Infection efficiency of retroviruses. After 2 days of RANKL stimulation, the efficiency of infection was determined by assaying ZsGreen expression with flow cytometry (left panel) or fluorescence microscopy (right panel). (C) The mRNA expression of *Klra17* (encoding Ly49Q) in osteoclast precursor cells transduced with retroviral vectors expressing shLy49Q (quantitative RT-PCR). Total RNA was isolated on the indicated days. The level of mRNA expression was normalized with *Gapdh* expression. (D) The effect of the retrovirus-mediated introduction of the shRNA for Ly49Q on RANKL-induced osteoclastogenesis.

***$P < 0.001$; n.s., not significant, throughout the paper). All data are expressed as means ± SEM.

Results

Selective expression of Ly49Q during osteoclast differentiation

The expression of Ly49 family receptors during osteoclast differentiation induced by RANKL and M-CSF was analyzed by GeneChip analysis (Fig. 1A). Among the Ly49 family receptors, *Klra17* (encoding Ly49Q) was highly and selectively induced during osteoclastogenesis. The protein expression of Ly49Q in BMMs was confirmed by flow cytometric analysis (Fig. 1B). In addition, the expression of *Klra17*, but not *Klra3* (encoding Ly49C), was markedly reduced by FK506, an inhibitor of calcineurin, suggesting that the induction of Ly49Q is dependent on the calcineurin–NFAT pathway (Fig. 1C). On the other hand, Ly49Q was not induced in calvarial osteoblasts treated with 1α, $25(OH)_2D_3$, and prostaglandin E_2 (PGE_2), which support osteoclast differentiation, or when cultured in an osteogenic medium which induces osteoblast differentiation (Fig. 1D). These results prompted us to examine the role of Ly49Q in osteoclastogenesis.

Inhibition of osteoclast differentiation by RNA interference (RNAi)-mediated knockdown of Ly49Q

To assess the role of Ly49Q during osteoclastogenesis, we performed RNAi-mediated knockdown of Ly49Q in the osteoclastogenesis induced by RANKL and M-CSF, using the retroviral short hairpin RNA (shRNA) delivery system (Fig. 2A). The infection efficiency was determined by analyzing the expression of ZsGreen, a green fluorescent protein encoded by the retrovirus vector, using flow cytometry. BMMs were transduced with retroviral vectors expressing shRNA targeting two different regions of Ly49Q (shLy49Q-1 and shLy49Q-2). As shown in Fig. 2B, more than 60% of the cells were positive for ZsGreen, indicating that shRNA-expressing retroviral vectors were efficiently transduced into BMMs. The mRNA expression of *Klra17* in osteoclast precursor cells was analyzed by quantitative RT-PCR, and was found to be significantly reduced by shLy49Q-1 as well as shLy49Q-2 (Fig. 2C). When the expression of NFATc1, the key transcription factor for osteoclastogenesis, was suppressed by shRNA targeting NFATc1 (shNFATc1), osteoclast differentiation was markedly inhibited (Fig. 2D). Based on previous studies [15–18], the ITIM-containing receptors negatively regulate osteoclastogenesis, but contrary to our expectation, the knockdown of Ly49Q significantly suppressed, rather than enhanced, the formation of the TRAP-positive multinucleated cells (MNCs) induced by RANKL and M-CSF (Fig. 2D). The difference in the inhibitory effects of shLy49Q-1 and shLy49Q-2 may result from the difference in the knockdown efficiency (see Fig. 2C). These results suggest that Ly49Q is a positive regulator of osteoclastogenesis, even though Ly49Q contains an ITIM motif.

Ly49Q as a positive regulator of osteoclast differentiation

Given our observation that the knockdown of Ly49Q resulted in the inhibition of RANKL-induced osteoclastogenesis, we investigated the expression of genes implicated in osteoclast differentiation and function by quantitative RT-PCR (Fig. 3A). Although the mRNA expression of *Tnfrsf11a*, *Csf1r*, or *Fos* was not changed by the Ly49Q knockdown, the expression levels of *Ctsk*, *Acp5*, *Oscar*, and *Tm7sf4* (encoding dendritic cell-specific transmembrane protein, DC-STAMP) were significantly decreased as compared to control. In addition, *Nfatc1* expression was potently suppressed by Ly49Q knockdown. Similar results were obtained with immunoblot analysis (Fig. 3B).

It is well documented that ITAM-mediated calcium signaling is crucial for the robust induction of NFATc1 during osteoclastogenesis [1,8]. Thus, it is likely that Ly49Q contributes to the activation of the calcium signaling, but how does an ITIM-bearing receptor stimulate calcium signaling? In the regulation of paired immunoglobulin-like receptors, negative regulation usually occurs in the presence of the activatory receptor recognizing the common ligands [11]. We therefore hypothesized that Ly49Q does not func-

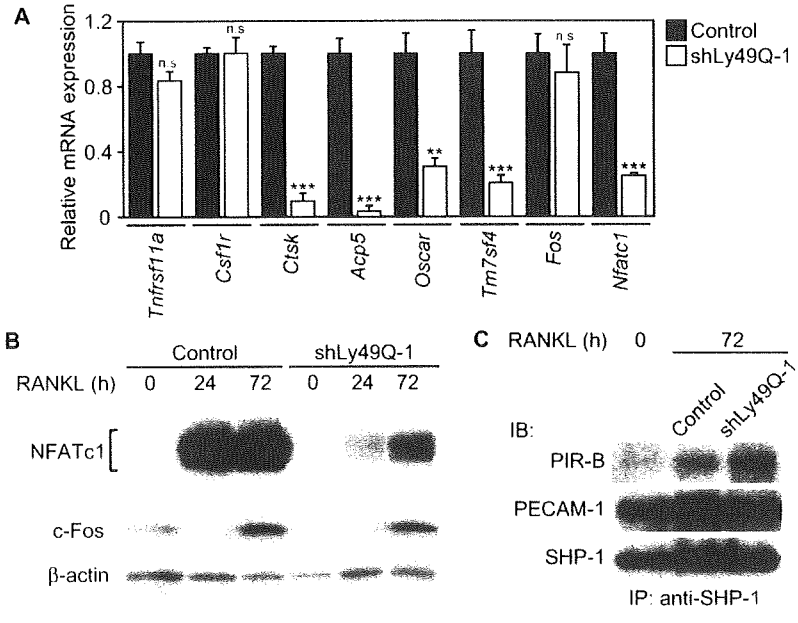

Fig. 3. Role of Ly49Q in RANKL-induced osteoclast differentiation. (A) Effect of Ly49Q knockdown on osteoclast-related gene expression (quantitative RT-PCR analysis). BMMs infected with retroviral vectors expressing control shRNA or shLy49Q-1 were cultured for 3 days with RANKL and M-CSF. (B) Effect of the Ly49Q knockdown on protein expression of NFATc1 and c-Fos (immunoblot analysis). (C) Effect of the Ly49Q knockdown on the association of SHP-1 with PIR-B or PECAM-1 in osteoclasts.

tion as a negative regulator, due to the lack of a corresponding activating receptor in the osteoclast lineage, and that Ly49Q efficiently associates with SHP-1 to deprive other ITIM-bearing inhibitory receptors of SHP-1, thus disabling the negative regulation. In fact, the association of SHP-1 with PIR-B, but not PECAM-1, was enhanced by the knockdown of Ly49Q (Fig. 3C). This result suggests that Ly49Q competes with PIR-B for the association of SHP-1, thereby functioning as a suppressor of PIR-B-mediated inhibitory effect on osteoclastogenesis.

Analysis of Ly49Q-deficient mice

We analyzed *in vitro* osteoclast differentiation in BMMs derived from Ly49Q-deficient mice. The formation of the TRAP-positive MNCs induced by RANKL and M-CSF was significantly reduced in the Ly49Q-deficient cells as compared with the wild-type (WT) cells (Fig. 4A). To evaluate the number of osteoblast progenitors in bone marrow, we performed a colony formation assay. The numbers of alkaline phosphatase-positive colony-forming unit-fibroblast (CFU-F) and von Kossa-positive CFU-osteoblast (CFU-OB) colonies in the culture of bone marrow cells were comparable in the WT and Ly49Q-deficient mice (data not shown). These results suggest that Ly49Q positively regulates osteoclast differentiation, without affecting osteoblastic bone formation.

Finally, to elucidate the role of Ly49Q *in vivo*, we analyzed the bone phenotype of Ly49Q-deficient mice. Unexpectedly, microCT analysis indicated no apparent difference between Ly49Q-deficient mice and WT littermates (Fig. 4B). For example, there was no difference in trabecular bone volume between the Ly49Q-deficient mice and WT littermates (Fig. 4D). Bone morphometric analysis also indicated no significant difference in osteoclast surface or osteoclast number in the metaphyseal region of the tibia (Fig. 4C and D). Similarly, the eroded surface was unchanged, suggesting that the osteoclastic bone resorption in Ly49Q-deficient mice was normal (Fig. 4D). Osteoblastic parameters, including osteoblast surface, osteoid surface, and osteoid volume, were comparable (data not shown). These results demonstrate that Ly49Q deficiency does not significantly influence osteoclast differentiation and function *in vivo* under physiological conditions.

Discussion

The crucial role of ITAM-bearing adaptors that associate with immunoglobulin-like receptors in osteoclast differentiation has

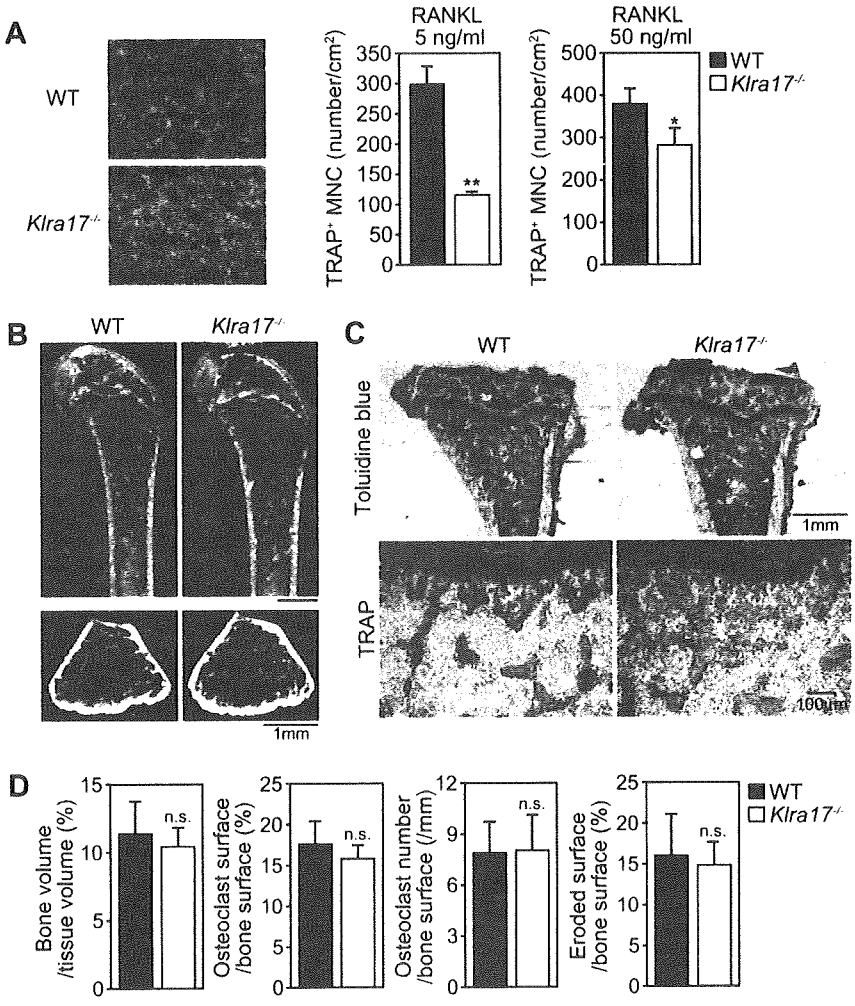

Fig. 4. Bone phenotype of Ly49Q-deficient (*Klra17*$^{-/-}$) mice. (A) Osteoclast differentiation in WT and Ly49Q-deficient BMMs stimulated with 5 and 50 ng/ml of RANKL in the presence of M-CSF. (B) MicroCT analysis of the femora of WT and Ly49Q-deficient mice (upper photograph: longitudinal view; lower photograph: axial view of the metaphyseal region). (C) Histological analysis of the proximal tibiae of WT and Ly49Q-deficient mice (upper photograph: toluidine blue staining; lower photograph: TRAP staining). (D) Bone volume determined by microCT analysis and osteoclastic parameters measured by bone morphometric analysis of WT and Ly49Q-deficient mice at the age of 9–10 weeks ($n = 4$).

been established [1,10]. However, the function of ITIM-bearing receptors has not been well understood. In the present report, we investigated the role of the ITIM-bearing NK receptor Ly49Q in osteoclastogenesis, because Ly49Q is specifically induced by RANKL stimulation in BMMs. Among NFAT family members, NFATc1 functions as the essential regulator for osteoclastogenesis [1,6] by inducing a number of genes which are involved in osteoclast differentiation and function [1,7]. We showed the RANKL-induced expression of Ly49Q, is dependent on the calcineurin–NFAT pathway, suggesting that Ly49Q induction is closely connected with the gene induction program activated during osteoclastogenesis. Interestingly, Ly49Q positively regulates *in vitro* osteoclastogenesis, unlike other ITIM-bearing receptors [15–18].

We explored the mechanisms underlying the positive regulation of osteoclast formation by an ITIM-bearing receptor. Since the expression level of SHP-1 is not changed by RANKL stimulation, it is likely that Ly49Q competes with other ITIM-bearing receptors for the recruitment of the limited amount of SHP-1 protein available during osteoclastogenesis. As shown in Fig. 3C, the recruitment of SHP-1 to PIR-B increased in the absence of Ly49Q. It is thus possible that the positive regulation by Ly49Q is based on the competition between Ly49Q and PIR-B, the latter of which is known to inhibit osteoclastogenesis through SHP-1. In the reported examples of the paired receptor system, the inhibitory receptor usually exerts its negative function in the presence of a corresponding activatory receptor and common ligands. Although the detailed mechanisms remain to be identified, Ly49Q may not be functional, possibly due to the lack of a corresponding activatory receptor in osteoclast precursor cells. Recent reports demonstrated that other ITIM-bearing receptors convey positive signals. For example, TREM-like transcript-1 (TLT-1), an ITIM-bearing receptor expressed on platelets, enhances calcium signaling by facilitating the recruitment of SHP-2 to the ITIM motif [28]. More recently, we demonstrated that Ly49Q promotes rapid polarization of neutrophils and tissue inflammation in the presence of inflammatory stimuli, although Ly49Q inhibits the adhesion and spreading of neutrophils at steady state [29]. These dual function of Ly49Q in neutrophils appeared to be mediated by changing the effecter phosphatase from SHP-1 to SHP-2 [29]. However, the role of SHP-2 in osteoclasts is still unknown and an important subject for future research.

In contrast to the *in vitro* observation, however, these results show a lack of an overt bone phenotype in Ly49Q-deficient mice. The role of Ly49Q may thus be compensated by other molecules *in vivo*. Indeed, mice lacking ITIM-bearing receptors, including PIR-B-deficient and SIRPα-mutant mice, also displayed a normal or subtly altered bone phenotype [15,16], suggesting that the ITIM-bearing receptor system is redundant. However, it has been shown that the expression of the MHC class I molecule, the ligand for Ly49Q, is induced by inflammatory cytokines such as TNF-α [30]. Therefore, it is possible that Ly49Q has a role in the enhanced osteoclastogenesis which occurs under various pathological conditions, including rheumatoid arthritis. This study provides an interesting example in which an ITIM-bearing receptor functions as a positive regulator of osteoclast differentiation and suggests a greater functional complexity of paired receptor systems than previously appreciated.

Acknowledgments

The authors thank T. Kitamura for providing Plat-E cell line. The authors also thank S. Sasawatari, T. Ando, Y. Kunisawa, M. and K. Nishikawa for reagents, discussion and technical assistance. This work was supported in part by a grant for ERATO, Takayanagi Osteonetwork Project from Japan Science and Technology Agency; Grant-in-Aids for Creative Scientific Research, Young Scientist (A) and Exploratory Research from the Japan Society for the Promotion of Science (JSPS); grants for the Genome Network Project and Global Center of Excellence Program from the Ministry of Education, Culture, Sports, Science and Technology of Japan (MEXT); and grants from Tokyo Biochemical Research Foundation, Life Science foundation of Japan, Yokoyama Foundation for Clinical Pharmacology, Takeda Science Foundation, Uehara Memorial Foundation, Nakatomi Foundation, Nagao Memorial Foundation, Kowa Life Science Foundation, Naito Foundation, Senri Life Science Foundation and Astellas Foundation for Research on Metabolic Disorders.

References

[1] H. Takayanagi, Osteoimmunology: shared mechanisms and crosstalk between the immune and bone systems, Nat. Rev. Immunol. 7 (2007) 292–304.
[2] T. Suda, N. Takahashi, N. Udagawa, E. Jimi, M.T. Gillespie, T.J. Martin, Modulation of osteoclast differentiation and function by the new members of the tumor necrosis factor receptor and ligand families, Endocr. Rev. 20 (1999) 345–357.
[3] H. Takayanagi, Osteoimmunology and the effects of the immune system on bone, Nat. Rev. Rheumatol. 5 (2009) 667–676.
[4] P. Chavassieux, E. Seeman, P.D. Delmas, Insights into material and structural basis of bone fragility from diseases associated with fractures: how determinants of the biomechanical properties of bone are compromised by disease, Endocr. Rev. 28 (2007) 151–164.
[5] S.L. Teitelbaum, F.P. Ross, Genetic regulation of osteoclast development and function, Nat. Rev. Genet. 4 (2003) 638–649.
[6] H. Takayanagi, S. Kim, T. Koga, H. Nishina, M. Isshiki, H. Yoshida, A. Saiura, M. Isobe, T. Yokochi, J. Inoue, E.F. Wagner, T.W. Mak, T. Kodama, T. Taniguchi, Induction and activation of the transcription factor NFATc1 (NFAT2) integrate RANKL signaling in terminal differentiation of osteoclasts, Dev. Cell 3 (2002) 889–901.
[7] T. Nakashima, H. Takayanagi, Osteoimmunology: crosstalk between the immune and bone systems, J. Clin. Immunol. 29 (2009) 555–567.
[8] T. Koga, M. Inui, K. Inoue, S. Kim, A. Suematsu, E. Kobayashi, T. Iwata, H. Ohnishi, T. Matozaki, T. Kodama, T. Taniguchi, H. Takayanagi, T. Takai, Costimulatory signals mediated by the ITAM motif cooperate with RANKL for bone homeostasis, Nature 428 (2004) 758–763.
[9] A. Mocsai, M.B. Humphrey, J.A. Van Ziffle, Y. Hu, A. Burghardt, S.C. Spusta, S. Majumdar, L.L. Lanier, C.A. Lowell, M.C. Nakamura, The immunomodulatory adapter proteins DAP12 and Fc receptor γ-chain (FcRγ) regulate development of functional osteoclasts through the Syk tyrosine kinase, Proc. Natl. Acad. Sci. USA 101 (2004) 6158–6163.
[10] M.C. Walsh, N. Kim, Y. Kadono, J. Rho, S.Y. Lee, J. Lorenzo, Y. Choi, Osteoimmunology: interplay between the immune system and bone metabolism, Annu. Rev. Immunol. 24 (2006) 33–63.
[11] J.V. Ravetch, L.L. Lanier, Immune inhibitory receptors, Science 290 (2000) 84–89.
[12] A. Veillette, S. Latour, D. Davidson, Negative regulation of immunoreceptor signaling, Annu. Rev. Immunol. 20 (2002) 669–707.
[13] S. Umeda, W.G. Beamer, K. Takagi, M. Naito, S. Hayashi, H. Yonemitsu, T. Yi, L.D. Shultz, Deficiency of SHP-1 protein-tyrosine phosphatase activity results in heightened osteoclast function and decreased bone density, Am. J. Pathol. 155 (1999) 223–233.
[14] K. Aoki, E. Didomenico, N.A. Sims, K. Mukhopadhyay, L. Neff, A. Houghton, M. Amling, J.B. Levy, W.C. Horne, R. Baron, The tyrosine phosphatase SHP-1 is a negative regulator of osteoclastogenesis and osteoclast resorbing activity: increased resorption and osteopenia in me^{v}/me^{v} mutant mice, Bone 25 (1999) 261–267.
[15] Y. Mori, S. Tsuji, M. Inui, Y. Sakamoto, S. Endo, Y. Ito, S. Fujimura, T. Koga, A. Nakamura, H. Takayanagi, E. Itoi, T. Takai, Inhibitory immunoglobulin-like receptors LILRB and PIR-B negatively regulate osteoclast development, J. Immunol. 181 (2008) 4742–4751.
[16] E.M. van Beek, T.J. de Vries, L. Mulder, T. Schoenmaker, K.A. Hoeben, T. Matozaki, G.E. Langenbach, G. Kraal, V. Everts, T.K. van den Berg, Inhibitory regulation of osteoclast bone resorption by signal regulatory protein α, FASEB J. 23 (2009) 4081–4090.
[17] Y. Wu, K. Tworkoski, M. Michaud, J.A. Madri, Bone marrow monocyte PECAM-1 deficiency elicits increased osteoclastogenesis resulting in trabecular bone loss, J. Immunol. 182 (2009) 2672–2679.
[18] D.H. Chung, M.B. Humphrey, M.C. Nakamura, D.G. Ginzinger, W.E. Seaman, M.R. Daws, CMRF-35-like molecule-1, a novel mouse myeloid receptor, can inhibit osteoclast formation, J. Immunol. 171 (2003) 6541–6548.
[19] S.K. Anderson, J.R. Ortaldo, D.W. McVicar, The ever-expanding Ly49 gene family: repertoire and signaling, Immunol. Rev. 181 (2001) 79–89.
[20] N. Toyama-Sorimachi, Y. Tsujimura, M. Maruya, A. Onoda, T. Kubota, S. Koyasu, K. Inaba, H. Karasuyama, Ly49Q, a member of the Ly49 family that is selectively expressed on myeloid lineage cells and involved in regulation of cytoskeletal architecture, Proc. Natl. Acad. Sci. USA 101 (2004) 1016–1021.
[21] N. Toyama-Sorimachi, Y. Omatsu, A. Onoda, Y. Tsujimura, T. Iyoda, A. Kikuchi-Maki, H. Sorimachi, T. Dohi, S. Taki, K. Inaba, H. Karasuyama, Inhibitory NK receptor Ly49Q is expressed on subsets of dendritic cells in a cellular

maturation- and cytokine stimulation-dependent manner, J. Immunol. 174 (2005) 4621–4629.
[22] M. Yoshizaki, A. Tazawa, E. Kasumi, S. Sasawatari, K. Itoh, T. Dohi, T. Sasazuki, K. Inaba, A.P. Makrigiannis, N. Toyama-Sorimachi, Spatiotemporal regulation of intracellular trafficking of Toll-like receptor 9 by an inhibitory receptor, Ly49Q, Blood 114 (2009) 1518–1527.
[23] M.C. Nakamura, E.C. Niemi, M.J. Fisher, L.D. Shultz, W.E. Seaman, J.C. Ryan, Mouse Ly-49A interrupts early signaling events in natural killer cell cytotoxicity and functionally associates with the SHP-1 tyrosine phosphatase, J. Exp. Med. 185 (1997) 673–684.
[24] L.H. Tai, M.L. Goulet, S. Belanger, N. Toyama-Sorimachi, N. Fodil-Cornu, S.M. Vidal, A.D. Troke, D.W. McVicar, A.P. Makrigiannis, Positive regulation of plasmacytoid dendritic cell function via Ly49Q recognition of class I MHC, J. Exp. Med. 205 (2008) 3187–3199.
[25] M. Shinohara, T. Koga, K. Okamoto, S. Sakaguchi, K. Arai, H. Yasuda, T. Takai, T. Kodama, T. Morio, R.S. Geha, D. Kitamura, T. Kurosaki, W. Ellmeier, H. Takayanagi, Tyrosine kinases Btk and Tec regulate osteoclast differentiation by linking RANK and ITAM signals, Cell 132 (2008) 794–806.
[26] K. Sato, A. Suematsu, T. Nakashima, S. Takemoto-Kimura, K. Aoki, Y. Morishita, H. Asahara, K. Ohya, A. Yamaguchi, T. Takai, T. Kodama, T.A. Chatila, H. Bito, H. Takayanagi, Regulation of osteoclast differentiation and function by the CaMK-CREB pathway, Nat. Med. 12 (2006) 1410–1416.
[27] T. Koga, Y. Matsui, M. Asagiri, T. Kodama, B. de Crombrugghe, K. Nakashima, H. Takayanagi, NFAT and Osterix cooperatively regulate bone formation, Nat. Med. 11 (2005) 880–885.
[28] A.D. Barrow, E. Astoul, A. Floto, G. Brooke, I.A. Relou, N.S. Jennings, K.G. Smith, W. Ouwehand, R.W. Farndale, D.R. Alexander, J. Trowsdale, Cutting edge: TREM-like transcript-1, a platelet immunoreceptor tyrosine-based inhibition motif encoding costimulatory immunoreceptor that enhances, rather than inhibits, calcium signaling via SHP-2, J. Immunol. 172 (2004) 5838–5842.
[29] S. Sasawatari, M. Yoshizaki, C. Taya, A. Tazawa, K. Furuyama-Tanaka, H. Yonekawa, T. Dohi, A.P. Makrigiannis, T. Sasazuki, K. Inaba, N. Toyama-Sorimachi, Ly49Q plays a crucial role in neutrophil polarization and migration by regulating raft trafficking, Immunity, in press. doi:10.1016/j.immuni.2010.01.012.
[30] S. Ochi, M. Shinohara, K. Sato, H.J. Gober, T. Koga, T. Kodama, T. Takai, N. Miyasaka, H. Takayanagi, Pathological role of osteoclast costimulation in arthritis-induced bone loss, Proc. Natl. Acad. Sci. USA 104 (2007) 11394–11399.

Gasp, a Grb2-associating protein, is critical for positive selection of thymocytes

Michael S. Patrick[a,b,1], Hiroyo Oda[a,1], Kunihiro Hayakawa[a], Yoshinori Sato[a], Koji Eshima[c], Teruo Kirikae[d], Shun-ichiro Iemura[e], Mutsunori Shirai[b], Takaya Abe[f], Tohru Natsume[e], Takehiko Sasazuki[g], and Harumi Suzuki[a,2]

Departments of [a]Pathology and [d]Infectious Diseases, International Medical Center of Japan, 1-21-1 Toyama, Shinjuku, Tokyo 162-8655 Japan; [b]Department of Microbiology, Yamaguchi University School of Medicine, 1-1-1 Minami-Kogushi, Ube, Yamaguchi 755-8505 Japan; [c]Department of Immunology, Kitasato University School of Medicine, 1-15-1 Kitasato, Sagamihara, Kanagawa 228-8555 Japan; [e]National Institute of Advanced Industrial Science and Technology, Biological Information Research Center, 2-42 Aomi, Kohtoh-ku, Tokyo 135-0064 Japan; [f]Laboratory for Animal Resources and Genetic Engineering, Center for Developmental Biology, RIKEN, 2-2-3 Minatojima Minami, Chuou-ku, Kobe 65-0047 Japan; and [g]International Medical Center of Japan, 1-21-1 Toyama, Shinjuku, Tokyo 162-8655, Japan

Communicated by Tadamitsu Kishimoto, Osaka University, Osaka, Japan, July 31, 2009 (received for review June 11, 2009)

T cells develop in the thymus through positive and negative selection, which are responsible for shaping the T cell receptor (TCR) repertoire. To elucidate the molecular mechanisms involved in selection remains an area of intense interest. Here, we identified and characterized a gene product Gasp (Grb2-associating protein, also called Themis) that is critically required for positive selection. Gasp is a cytosolic protein with no known functional motifs that is expressed only in T cells, especially immature CD4/CD8 double positive (DP) thymocytes. In the absence of Gasp, differentiation of both CD4 and CD8 single positive cells in the thymus was severely inhibited, whereas all other TCR-induced events such as β-selection, negative selection, peripheral activation, and homeostatic proliferation were unaffected. We found that Gasp constitutively associates with Grb2 via its N-terminal Src homology 3 domain, suggesting that Gasp acts as a thymocyte-specific adaptor for Grb2 or regulates Ras signaling in DP thymocytes. Collectively, we have described a gene called Gasp that is critical for positive selection.

differentiation | signal transduction | T cell receptor | thymus

Development of conventional T cell receptor (TCR)-αβ T cells in the thymus requires multiple stages defined by the expression pattern of CD4 and CD8 coreceptor molecules. The most immature $CD4^-CD8^-$ [double negative (DN)] thymocytes differentiate to the $CD4^+CD8^+$ [double positive (DP)] stage through the first selection process called β-selection (pre-TCR selection). These DP thymocytes are subjected to both positive and negative selection to become either class II MHC-restricted helper $CD4^+CD8^-$ [CD4-single positive (CD4-SP)] or class I MHC-restricted cytotoxic $CD4^-CD8^+$ (CD8-SP) cells (1). After receiving positive selection signals, DP thymocytes go through an intermediate $CD4^+CD8^{lo}$ stage, irrespective of their lineage decision (2). The fate of individual DP thymocytes is determined by the strength of affinity and longevity of interaction between their TCR and peptide:MHC ligand (3). Although it is known that strong TCR/ligand interaction leads to negative selection and weak association results in positive selection (4), how this quantitative difference of TCR interaction can be converted to the qualitative difference is not known. Therefore, it is important to investigate the difference in molecular mechanisms of positive and negative selection.

One of the widely accepted models for explaining the difference between positive and negative selection is differential MAPK activation (5). Initially, differential requirements for ERK in positive selection and JNK/p38 in negative selection were focused on (6). The guanine nucleotide exchange factor (GEF) Sos has dual activity for Ras and Rac, therefore it can activate both the ERK and JNK/p38 pathways. Recently, RasGRP, which is another GEF for Ras, was shown to be critical for positive but not negative selection (7). Furthermore, mice heterozygous for Grb2, which constitutively associates with Sos, showed inefficient JNK/p38 activation, but normal ERK activation (8). From these results, positive selection signals were thought to induce the RasGRP/Ras/ERK pathway, and negative selection signals were thought to induce the Grb2-Sos/Rac/JNK p38 pathway. The model that activation through RasGRP results in weak sustained ERK activation to induce positive selection, whereas activation through Sos induces strong temporary ERK activation leading to negative selection is still widely accepted (9). Recently, Daniels et al. (10) elegantly showed that positive selection signals induced subcellular compartmentalization of RasGRP/Ras/ERK to the Golgi membrane, whereas negative selection signals induced localization of Grb2-Sos/Ras/ERK to the plasma membrane. Furthermore, positive selector-induced ERK activation lasted longer in Golgi than in the plasma membrane. Therefore, subcellular compartmentalization of Ras-GEF and Ras upon TCR stimulation is now widely accepted to be the branch point of positive and negative selection (11).

To find novel genes involved in the positive selection of thymocytes, we tried to isolate unknown genes whose expression is highly restricted to the thymus, the site where selection takes place. We used EST databases and performed in silico cloning, the strategy successfully used for isolating various novel tissue or cell type-specific genes. We selected several "thymus-specific genes" by our own computer algorithm based on their thymus-restricted expression. Among these thymus-specific genes, we focused on one gene E430004N04Rik (GeneID 210757), mainly because of its exclusive expression in immature DP thymocytes. Because we found that this protein constitutively associates with Grb2, we called the gene Gasp (Grb2-associating protein). Gasp contains no known protein motifs or homology domain and has no known function, although it has well conserved orthologs in multiple vertebrates from fish to human. To elucidate the function of Gasp, we established *Gasp*-deficient mice and found that the gene is critical for positive selection but not for other TCR-mediated signaling events.

Results

Expression of Gasp Protein. To identify novel genes specifically expressed in the thymus, we used information from the National Center for Biotechnology Information Unigene database of expressed sequence tags (ESTs). Each Unigene cluster contains information about the number of EST clones from a tissue source. We searched Unigene clusters based on the proportion of clones derived from thymus and total number of clones from the thymus. Finally, we selected five genes as thymus-specific genes. The gene Gasp (E430004N04Rik, Themis, Tsepa) was one of these thymus-specific genes. We first examined the expression of Gasp in various

Author contributions: T.S. and H.S. designed research; M.S.P., H.O., K.H., Y.S., K.E., S.-i.I., M.S., and T.N. performed research; T.K. and T.A. contributed new reagents/analytic tools; M.S.P., H.O., K.E., S.-i.I., T.N., and H.S. analyzed data; and M.S.P. and H.S. wrote the paper.

The authors declare no conflict of interest.

[1]M.S.P. and H.O. contributed equally to this work.

[2]To whom correspondence should be addressed. E-mail: hsuzuki@ri.imcj.go.jp.

This article contains supporting information online at www.pnas.org/cgi/content/full/0908593106/DCSupplemental.

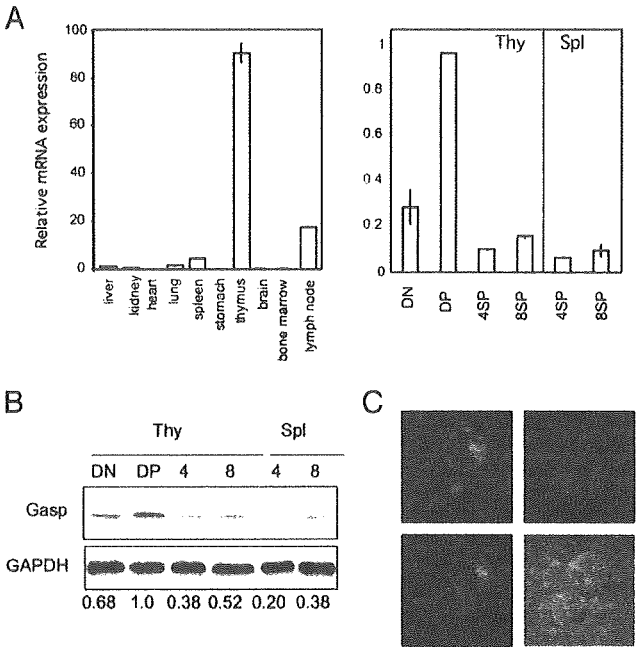

Fig. 1. Thymus-specific expression of Gasp. (*A*) Expression of Gasp mRNA was analyzed by real-time PCR from C57BL/6 mouse tissues and cells. RNA expression was normalized relative to β-actin. Error bars are the SD ($n = 2$ and 3). (*B*) Expression of Gasp protein in sorted thymic or splenic T cell subpopulations. Results are representative of two independent experiments. (*C*) Representative micrograph showing subcellular localization of Gasp. GFP-fused Gasp was exogenously introduced in DPK cell line (green) and costained with DAPI (blue). (Magnification: ×1,000.)

tissues and cells. As expected, mRNA expression of Gasp is highly restricted to lymphoid organs, especially in the thymus and T cells (Fig. 1*A*). Among T cell subsets, expression is highest in DP thymocytes, and its expression decreases along with maturation. The same pattern of protein expression was confirmed by Western blot analysis using Gasp-specific antibody (Fig. 1*B*). Expression of the gene in CD8-SP cells is slightly higher than in CD4-SP cells in both the thymus and spleen. Expression of Gasp in Treg cells was lower than in conventional CD4 T cells, consistent with a previous report describing Gasp as one of the most reduced genes in Tregs by comprehensive microarray analysis (12). Transcription of Gasp was not affected upon stimulation with phorbol 12-myristate 13-acetate (PMA) and ionomycin. Analysis by confocal microscopy of exogenously introduced GFP-fusion Gasp protein (both N- and C-terminal fusion protein) in a DP thymoma line (DPK) (13) showed homogeneous distribution in cytosol and exclusion from the nucleus (Fig. 1*C*). We did not observe a change in the distribution of GFP-fusion Gasp protein upon TCR stimulation.

Gasp Is Required for Positive Selection but Not for Negative Selection and β-Selection. To elucidate the precise function of Gasp, we generated *Gasp*-deficient mice by replacing the first exon of *Gasp* with a LacZ and Neo-expressing cassette (Fig. 2*A*). Protein expression of Gasp in $Gasp^{+/+}$, $Gasp^{+/-}$, and $Gasp^{-/-}$ thymocytes is shown in Fig. 2*B*, confirming the absence of Gasp protein in the deficient mice and reduced protein expression in $Gasp^{+/-}$ thymocytes. In thymi of $Gasp^{-/-}$ mice, total cell number was not significantly altered, and proportions of DN1 through DN4 in DN cells were normal, indicating that β-selection was unaffected in the mice (Table S1). However, we observed a marked decrease of CD4-SP and CD8-SP cells in the thymus (Fig. 2*C*). The effect of Gasp on positive selection is dose-dependent, because the phenotype of $Gasp^{+/-}$ mice was intermediate to that of $Gasp^{+/+}$ and $Gasp^{-/-}$ mice. Reduction of CD4-SP cells in the thymus can be observed even in the neonate, suggesting that the defect is a relatively early event in positive selection (Fig. 2*D*). To confirm the defect in positive selection, we next examined the developmental fate of thymocytes expressing three different fixed TCRs. DP thymocytes expressing class II-MHC restricted OT-II TCR transgenic (Tg) mice on a *RAG* null background did not differentiate into CD4-SP cells at all in the absence of Gasp (Fig. 2*E Top*). The class I-specific female HY-TCR Tg (14) $RAG^{-/-}$ thymocytes and OT-I TCR Tg thymocytes did not differentiate into CD8-SP cells either (Fig. 2*E Middle* and *Bottom*). Therefore, Gasp is critically required for positive selection of both thymocytes expressing class I- and class II-restricted TCR. We extensively analyzed various surface markers (e.g., CD2, CD5, HSA, CD25, class I MHC, etc.) of each stage of thymocyte development, but we did not observe significant differences between $Gasp^{+/+}$ and $Gasp^{-/-}$ thymocytes. The only difference we found was in the expression of CCR9 and CD62L (Fig. S1). Down-regulation of CCR9 on CD4-SP cells was not observed in $Gasp^{-/-}$ thymocytes, and the expression of CD62L on $Gasp^{-/-}$ CD4-SP cells was significantly decreased (Fig. S1). Differentiation of γδ-T cells in $Gasp^{-/-}$ mice was not altered (Table S1). By hematoxylin and eosin staining of thymus sections, no significant difference was observed in cortical and medullary architecture.

Because the above data show that Gasp is crucial in positive selection, we next investigated the effect of Gasp on negative selection, the other important TCR signal-initiated event. Contrary to the defect in positive selection, Gasp deficiency does not affect negative selection as the generation of DP was not recovered in the absence of Gasp in male HY-TCR Tg background (Fig. 2*F*).

***Gasp*$^{-/-}$ T Cells Expand in Periphery.** In contrast to severe impairment of positive selection in the thymus of $Gasp^{-/-}$ mice, the reduction of mature T cells in the periphery was much milder. In particular, reduction of CD8-SP cells was less significant and thus the reduction of CD4-SP cells is always severer than that in CD8-SP cells in $Gasp^{-/-}$ mice. It is noteworthy that the proportion of CD8-SP cells was even higher in $Gasp^{-/-}$ mesenteric lymph node (mLN) and inguinal lymph node (iLN) (Fig. 3*A*) compared with wild type. Because the total numbers of lymph node and spleen cells of $Gasp^{-/-}$ mice were fewer than wild type, absolute numbers of both CD4-SP and CD8-SP cells in spleen and lymph nodes were always less than in wild-type controls (Fig. 3*B*).

The less severe phenotype in number of peripheral T cells could be explained by homeostatic expansion of differentiated T cells. Therefore, we evaluated memory/activated phenotype of peripheral cells. As shown in Fig. 3*C*, CD4-SP cells in $Gasp^{-/-}$ mice contained many more memory/activated ($CD44^{hi}$ $CD62L^{-}$) phenotype cells than wild-type controls. CD8-SP cells also express CD44 at high levels, but somehow expression of CD62L was not reduced (Fig. 3*C*). Consistent with these activated phenotypes, both CD4-SP and CD8-SP cells in $Gasp^{-/-}$ mice showed significantly increased BrdU uptake in vivo, indicating that peripheral CD4-SP and CD8-SP cells in $Gasp^{-/-}$ mice proliferate without stimulation (Fig. 3*D*). Although such proliferation could be caused by autoreactive T cells, we did not see any signs of autoimmune disease in the deficient mice. We observed very few CD8-SP cells in the periphery of female HY-TCR Tg $RAG^{-/-}$, $Gasp^{-/-}$mice. Because it was reported that homeostatic proliferation does not occur in the periphery of female HY TCR-Tg mice (15), the results also support the model that the increased number of peripheral T cells in $Gasp^{-/-}$ mice was caused by homeostatic proliferation. From these results, we conclude that positive selection of CD4-SP and CD8-SP cells are both blocked in $Gasp^{-/-}$ mice, but the number of T cells in periphery is increased by homeostatic expansion.

Normal Activation of Mature *Gasp*$^{-/-}$ T Cells. We next investigated functions of peripheral T cells. Purified splenic CD4-SP cells ($CD4^{+}$, $CD8^{-}$, and $Mac1^{-}$ cells) were stimulated with immobilized

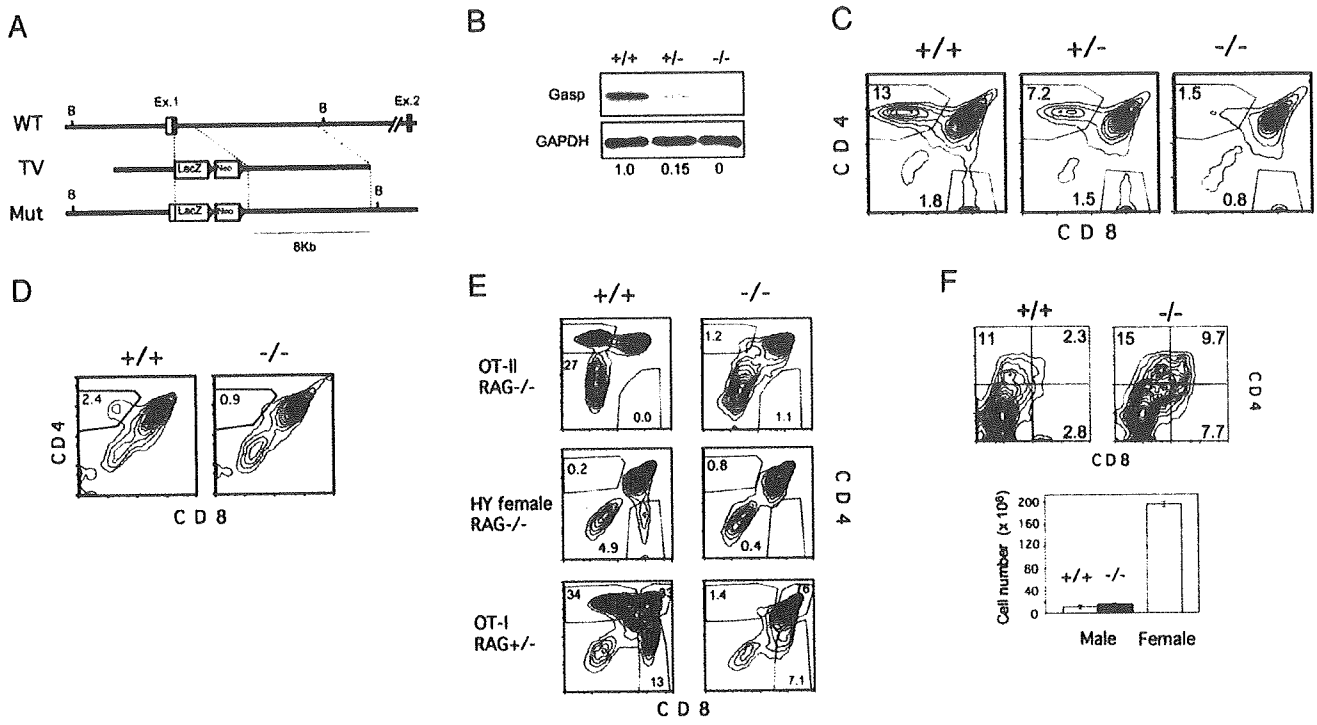

Fig. 2. Generation and analysis of *Gasp*$^{-/-}$mice. (*A*) A gene-targeting strategy was used to insert a lacZ/neo cassette into exon 1 of the Gasp gene. (*B*) Western blot analysis of DP thymocytes with anti-Gasp-specific antisera. Results are representative of two independent experiments. (*C*) CD4 and CD8 profile of *Gasp*$^{+/+}$, *Gasp*$^{+/-}$, and *Gasp*$^{-/-}$ thymocytes. (*D*) CD4 and CD8 expression of neonatal thymocytes. (*E*) CD4 and CD8 profile of thymocytes from OT-I, OT-II Tg *RAG*$^{-/-}$, and female HY Tg *RAG*$^{-/-}$mice. (*F*) CD4 and CD8 profile and number of thymocytes from male HY Tg *RAG*$^{-/-}$mice. In *C–F*, data are representative of more than three independent experiments.

anti-CD3 and CD28 antibodies in vitro, then measured for growth and IL-2 production. As shown in Fig. 4 *A* and *B*, TCR-dependent cell growth evaluated by 3-(4,5-dimethylthiazol-2-yl)-2,5-diphenyl tetrazolium bromide (MTT) assay and production of IL-2 in supernatant was comparable between *Gasp*$^{+/+}$ and *Gasp*$^{-/-}$ mice. We established alloantigen (H-2^d)-specific CD4-SP and CD8-SP T cell lines from wild-type and *Gasp*$^{-/-}$ splenocytes. Upon TCR stimulation, *Gasp*$^{-/-}$CD4-SP helper T cell lines produced amounts of IL-4 comparable to wild-type lines (Fig. 4*C Left*). CD8-SP CTL T cell lines produced the same amount of IFN-γ upon stimulation as wild types (Fig. 4*C Right*). We also measured CTL activity of these CD8-SP clones and found that specific killing of CD8-SP CTL clones against allogenic H-2^d MHC was not changed in the absence of Gasp (Fig. 4*D*). From these results, we conclude that activation of mature T cells does not require Gasp.

Phenotypes of *Gasp*$^{-/-}$ Thymocytes. We noticed that the phenotype of *Gasp*$^{-/-}$ mice was quite similar to *thid* (LEC) mutant rat (16). Those reports showed reduced numbers of CD4-SP cells, but not CD8-SP cells in lymph nodes (16), and lower expression of CD62L in CD4-SP cells (17), which are exactly the same phenotypes as *Gasp*$^{-/-}$ mice. The responsible gene for *thid* mutation was recently reported as *PTPRK* (protein tyrosine phosphatase receptor K) (18, 19), and the gene is only 100 Kb apart from the *Gasp* gene locus. To exclude the possibility that the disturbance of expression of the adjacent *PTPRK* gene was responsible for the phenotype of *Gasp*$^{-/-}$ mice, we analyzed expression of PTPRK mRNA in *Gasp*$^{-/-}$ thymocytes by real-time RT-PCR analysis. The expression of PTPRK is not reduced but rather increased in *Gasp*$^{-/-}$ thymocytes (Fig. 5*A*). Therefore, the phenotype of *Gasp*$^{-/-}$ mice is likely independent of PTPRK.

We next performed bone marrow chimera experiments to investigate whether the developmental defect in the thymus was caused by an intrinsic thymocyte defect or a defect in the thymic microenvironment. As shown in Fig. 5*B*, thymocytes from wild-type bone marrow developed normally in irradiated *Gasp*$^{-/-}$ mice, whereas wild-type mice reconstituted with *Gasp*$^{-/-}$ bone marrow showed almost identical phenotypes as *Gasp*$^{-/-}$ mice. Therefore, the defect is thymocyte intrinsic, which is consistent with the specific expression of Gasp in thymocytes (Fig. 1*A*).

We next analyzed the expression of TCR on thymocytes. Although TCR-β expression on CD4-SP cells in the thymus is consistently lower than wild type, expression of TCR on preselected DP and peripheral mature T cells (Fig. S2 *A* and *B*) were comparable to the wild type. Expression of TCR on DP thymocytes of TCR-Tg mice was also not significantly changed (Fig. S2*C*). Furthermore, spontaneous and TCR-induced cell death evaluated by AnnexinV staining was not significantly different in the absence of Gasp (Fig. S3).

Signal Transduction in *Gasp*$^{-/-}$ DP Cells. We next focused on the DP stage when positive selection takes place. We observed a significant reduction in the earliest postselected DP (CD69^{hi} TCR^{hi} DP) in *Gasp*$^{-/-}$mice (Fig. 5*C*), suggesting that the defect lies in a relatively early phase of the selection process. We next investigated TCR-stimulated signal transduction of DP thymocytes. Stimulation with plate-coated anti-CD3 plus CD28 antibody successfully induced CD69 up-regulation on *Gasp*$^{-/-}$DP thymocytes (Fig. 5*D*), indicating that the signaling pathway leading to CD69 transcription was not affected. In accordance with that, anti-CD3 mAb induced Ca^{2+} influx in DP thymocytes was not significantly disturbed (Fig. 5*E*). Furthermore, anti-CD3 mAb induced phosphorylation of ERK, phospholipase C γ (PLC-γ), and SLP76, all were unaltered in *Gasp*-deficient DP thymocytes (Fig. 5*F*).

Gasp Constitutively Associates with Grb2. To figure out the function of Gasp further, we attempted to identify proteins associated with

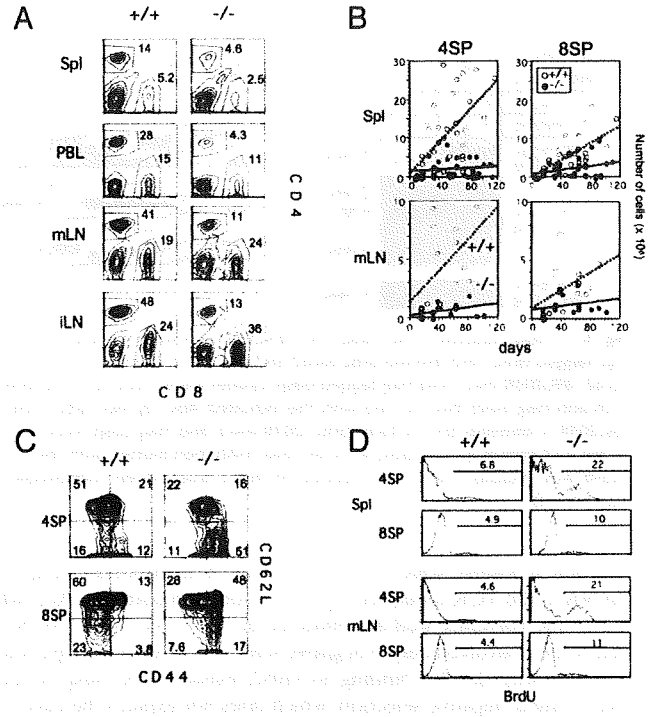

Fig. 3. Phenotype of peripheral T cells in *Gasp*$^{-/-}$ mice. (*A*) CD4 and CD8 profile of the cells from spleen, peripheral blood (PBL), mLN, and iLN of *Gasp*$^{+/+}$ and *Gasp*$^{-/-}$ mice. Results are representative of more than five independent experiments. (*B*) Absolute number of CD4-SP and CD8-SP cells of Spl and mLN of *Gasp*$^{+/+}$ and *Gasp*$^{-/-}$ mice. Each dot represents individual mice at day of age. Solid (−/−) and dashed (+/+) lines show the linear regression correlation between age and absolute number of cells. (*C*) CD44 and CD62L profile of splenic CD4-SP and CD8-SP cells from *Gasp*$^{+/+}$ and *Gasp*$^{-/-}$ mice. (*D*) BrdU uptake of CD4-SP and CD8-SP cells from spleen and mLN of *Gasp*$^{+/+}$ and *Gasp*$^{-/-}$ mice. After mice were fed with BrdU for 5 days with drinking water, the cells were stained with anti-BrdU antibody. In *C* and *D*, results are representative of more than three independent experiments.

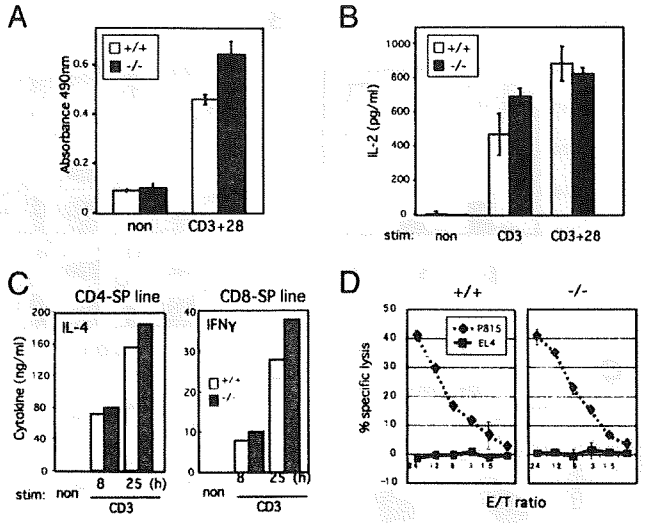

Fig. 4. Activation of peripheral CD4 and CD8 mature T cells. (*A*) MTT assay was applied for TCR-stimulated sorted splenic CD4-SP cells of *Gasp*$^{+/+}$ and *Gasp*$^{-/-}$ mice after 3 days of culture. (*B*) Primary CD4-SP T cells from *Gasp*$^{+/+}$ and *Gasp*$^{-/-}$ mice were stimulated with plate-bound anti-CD3 or CD3^{+} 28 mAb for 24 h, and IL-2 concentration in supernatants was measured by ELISA. (*C*) TCR-dependent production of IL4 and IFN-γ from cell line established from *Gasp*$^{+/+}$ and *Gasp*$^{-/-}$ splenocyte. (*D*) H-2^{d}-specific allo-CTL lines were established from splenic CD8-SP cells, and CTL assay was analyzed for CTL function by using specific (P815) and nonspecific (EL4). Results are representative of more than two independent experiments.

Gasp by using liquid chromatography-based electrospray tandem mass spectrometry (20). Human embryonic kidney cells were transfected with Flag-tagged human Gasp, and lysates from these cells were immunoprecipitated with anti-Flag antibody. Immunoprecipitated proteins were subjected to proteolysis followed by liquid chromatography-based electrospray tandem mass spectrometry. The analysis gave us several candidate Gasp-associating proteins. Among them, the most frequently detected amino acid sequences were derived from Grb2. Grb2 is an adaptor protein constitutively associated with Sos, having two Src homology 3 (SH3) domain (N and C terminus) and one SH2 domain in the middle (21). Therefore, we next performed coimmunoprecipitation experiments using Flag-tagged Gasp and myc-tagged Grb2 and their mutants. As shown in Fig. 6, myc-Grb2 could successfully pull down Flag-Gasp, and Flag-Gasp also coprecipitated myc-Grb2. Although a Grb2 mutant lacking the entire SH2 region (Grb2-ΔSH2) could associate with Gasp, an SH3 mutant (Grb2–42L/203R) in which both the N- and C-terminal SH3 domains were mutated (22) could not (Fig. 6). Because Grb2–203R in which only the C-terminal SH3 domain was mutated could associate with Gasp (Fig. 6*B*), Gasp likely associates with Grb2 via its N-terminal SH3 region, which is the same binding site for Sos (23). We noticed that Gasp contains a proline-rich sequence (^{555}PPPRPPKHP) in its C terminus. Although it is different from the consensus Grb2 SH3 domain binding sequence (PVPPPVPPR), we made a deletion mutant of this proline-rich sequence (HA-Gasp-ΔPro) and tested its interaction with Grb2. As shown in Fig. S4, we found that the association was independent of this proline-rich region. We also found Gasp was not tyrosine-phosphorylated upon TCR stimulation or PMA+ionomycin stimulation (Fig. S5), consistent with the observation that treatment with pervanadate did not augment the association of Gasp and Grb2.

Discussion

Although it is well known that both positive selection and negative selection are evoked by stimulation of TCRs of different affinities, the molecular basis of these selection processes is poorly understood. The molecules exclusively required for either selection process will give us a hint to figure out the molecular mechanism of these two selections. At present, ERK (24), Calcineurin (25), TCR-αcpm (26), and RasGRP (7) are described to be required only for positive selection but not for negative selection, whereas bim (26), MINK (27), and nur77 (28) are required only for negative selection. We have now added another gene to the list of players required for positive selection.

Gasp, which is preferentially expressed in immature DP thymocytes, has quite unique characteristics. Most of the proteins reported to be required for positive selection are involved in TCR-induced signal transduction. As a result, other TCR-related signaling events such as peripheral activation and homeostatic expansion are also affected. Unlike other positive selection-deficient mutant mice, *Gasp*$^{-/-}$ mice showed a defect only in positive selection among all of the TCR-induced signaling events. However, it should be noted that the male HY-TCR Tg system may not be appropriate for assessment of physiological negative selection because developmental arrest occurs before the DP stage (29).

In the periphery of *Gasp*$^{-/-}$ mice, the number of CD8-SP cells in lymph nodes was more than CD4-SP cells, suggesting some effect of Gasp on CD4/CD8 lineage choice. However, analysis of three independent TCR Tg mice clearly showed there is no lineage conversion nor incomplete block in positive selection of class I-restricted TCR.

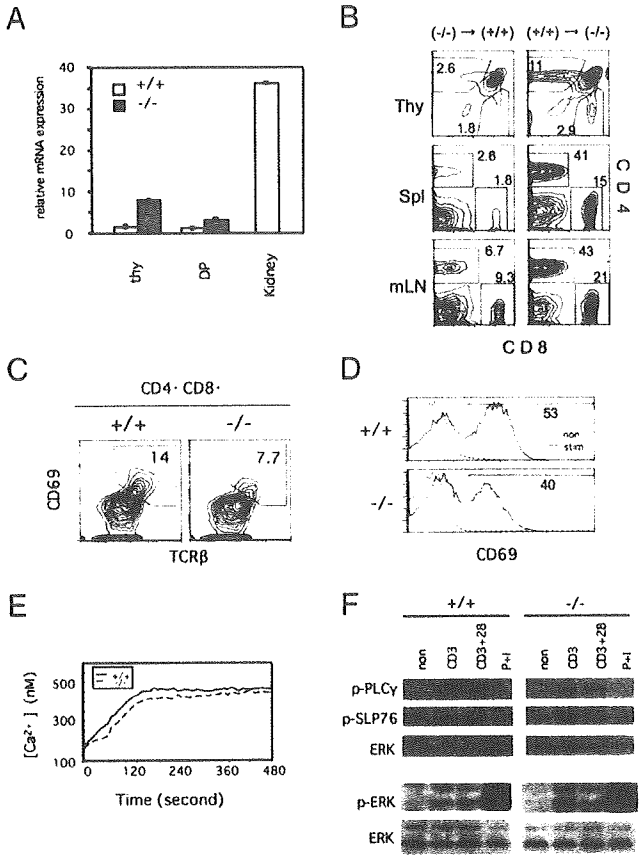

Fig. 5. Characteristics of Gasp deficiency. (*A*) Defects in *Gasp*$^{-/-}$ mice are independent of PTPRK. Expression of PTPRK mRNA in *Gasp*$^{-/-}$ thymocytes was determined by real-time RT-PCR. Error bars are the SD (n = 2 and 3). (*B*) Developmental defects in *Gasp*$^{-/-}$ mice are thymocyte intrinsic. Bone marrow cells from CD45.1 *Gasp*$^{+/+}$ mice were injected into lethally irradiated CD45.2 *Gasp*$^{-/-}$ mice or vice versa. After 2 months, cells from indicated organs were stained with CD4, 8, 45.1, and 45.2. Results are representative of more than two independent mice. (*C*) Proportion of post-selected CD69^{+} TCR^{hi} DP cells in *Gasp*$^{+/+}$ and *Gasp*$^{-/-}$ mice. Results are representative of four independent experiments. (*D*) Sorted DP thymocytes from *Gasp*$^{+/+}$ and *Gasp*$^{-/-}$ mice were activated with plate-bound CD3 + 28 Ab overnight, then stained with CD69. Results are representative of more than three independent experiments. (*E*) DP cells from *Gasp*$^{-/-}$ mice were stimulated with anti-CD3 mAb followed by anti-hamster IgG, then Ca^{2+} concentration was measured by using Fura2-AM. Results are representative of three independent experiments. (*F*) DP thymocytes were activated by the indicated stimuli (2 min for anti-CD3 and 3 + 28, 5 min for PMA + Iono), then Western blotted with phosphorylated-ERK-, SLP76-, and PLCγ-specific antibody. Results are representative of more than three independent experiments.

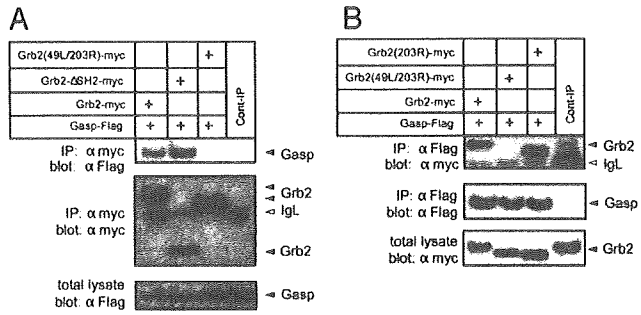

Fig. 6. Gasp associates with Grb2. (*A*) HEK293T cells were transfected with myc-tagged Grb2, SH2-deleted Grb2 (Grb2-SH2-myc), N-/C-terminal SH3 mutant (Grb2–49L/203R-myc), and Flag-tagged Gasp. Lysates were immunoprecipitated with anti-Flag mAb then blotted with the indicated Abs. (*B*) myc-Grb2, Grb2–49L/203R, C-terminal SH3 mutant (Grb2–203R-myc) ,and Flag-Gasp were transfected and immunoprecipitated with anti-myc mAb then blotted with the indicated Abs. Results are representative of more than seven independent experiments.

Reduction of CD69^{+} TCR^{hi}DP in *Gasp*$^{-/-}$ mice and the disappearance of CD4^{+} CD8^{hi} post-selected cells (2) in OT-I TCR Tg thymocytes also indicate that the defect in positive selection is relatively early and affects both CD4 and CD8 lineages. We found that a large part of peripheral *Gasp*$^{-/-}$ T cells are actively proliferating without antigenic stimulation, and that is why the peripheral phenotype of *Gasp*$^{-/-}$ mice is much milder than that in the thymus. Because we do not observe any signs of autoimmune symptom in even >1-year-old *Gasp*$^{-/-}$ mice, these proliferating T cells are not autoreactive, but expand by homeostatic proliferation. We always observed severer reductions in CD4-SP cells than CD8-SP cells in the periphery of *Gasp*$^{-/-}$ mice. Furthermore, higher expression of CD62L in Gasp$^{-/-}$ CD8-SP cells could explain preferential migration of CD8-SP cells into lymph nodes.

Our finding that Gasp constitutively associated with Grb2 is quite intriguing and provides some possible links to hypothesize its function in positive selection, because Grb2 is an important adaptor for Sos in the TCR-mediated signal transduction pathway. According to the currently well-accepted model (5, 9–11, 30), Grb2/Sos activation is involved only in negative selection. Because Gasp could compete with Sos for binding to Grb2, existence of Gasp would likely inhibit negative selection, which does not explain the current phenotype well. However, there is no direct evidence that Sos is required for thymic selection, because Sos1 deletion is embryonic lethal (31), and Sos2-deficient mice showed no phenotype (32). Although an earlier study using Grb2$^{-/-}$ mice suggested Grb2 is involved in negative selection but not in positive selection (8), recent results from lck-Cre driven Grb2 conditional deficient mice suggests that Grb2 is required for positive selection. According to these facts, Gasp is more likely to function as an adaptor for Grb2, bringing some unknown molecule required for positive selection to the LAT signalosome complex. If Gasp functions in TCR-mediated signal transduction, it is surprising that *Gasp*$^{-/-}$ DP thymocytes did not show any defect in signal transduction induced by various dose ranges (5–0.1 μg/mL) of anti-TCR antibody. However, it is still possible that *Gasp*$^{-/-}$ thymocytes have signaling defects when stimulated by weaker signals or physiological MHC/peptide ligands.

In conclusion, we found a Grb2-associating protein that is specifically expressed in the thymus and is critical in positive selection but not in other TCR-related signal transduction events. Detailed function of the protein in positive selection should be studied further.

We would like to note that, during the review process of this article, several other groups' reports describing the same gene under the name "*Themis*" were published (33–35, 40).

Materials and Methods

Mice. *Gasp*$^{-/-}$ mice (CDB0574K: www.cdb.riken.jp/arg/mutant%20mice%20list.html) were generated as described (36, 37). The first exon of *Gasp* was targeted by homologous recombination using vector backbone DT-A/LacZ/neo with 5′ and 3′ flanking arms of 4 and 8 kbp, respectively. Neomycin-selected ES cell lines were screened by PCR, and two independent mouse lines were established. Southern blot analysis confirmed target gene deletion. The two independent mouse lines showed identical phenotypes. OT-I, OT-II, and HY mice have been described (14). All mice were housed under specific pathogen-free conditions and used in accordance with International Medical Center of Japan institutional guidelines.

Real-Time RT-PCR. Total RNA was isolated from tissues or cells by using the RNeasy kit (Qiagen). cDNA generated by SuperScript III (Invitrogen) was analyzed by using primers for the indicated gene and the Platinum SYBR Green qPCR-UDG Supermix with ROX (Invitrogen). Results were normalized to β-actin expression levels. Primer sequences for Gasp, PTPRK, and β-actin are available on request.

Immunoprecipitations and Western Blot Analysis. Transfection and immunoprecipitation were performed as described (38) with the exception of using 0.05% Nonidet P-40 lysis buffer. Antibodies for Western blot analysis were against: pPLCγ-1, ERK, and pERK (Cell Signaling) and pSLP76 (BD Biosciences). Anti-Gasp-specific rabbit antiserum was generated by injection of recombinant full-length Gasp protein. Antibodies used for immunoprecipitations were: anti-myc (9E10), anti-HA (Roche), and anti-FLAG (M2, Sigma). Horseradish peroxidase-conjugated anti-IgG secondary antibodies against rabbit, rat, and mouse (GE Healthcare) were used with Lumiglo (Cell Signaling) substrate.

Plasmids and Recombinant DNAs. Full-length murine Gasp cDNA was PCR-cloned using IMAGE clone 40130002 (OpenBiosystems) as template into pcDNA3 vector to generate Gasp-HA. To generate Gasp-ΔPro-HA, the proline-rich sequence ^{555}PPPRPPKHP of Gasp was deleted by site-directed PCR mutagenesis. A BamHI and XbaI fragment from pSVEGrb49L or pSVEGrb49L/203R (kind gifts from Robert Weinberg, Whitehead Institute, Cambridge, MA) was cloned into to pcDNA3.1 to generate Grb2(203R)-myc and Grb2(49L/203R)-myc. Grb2-myc and Grb2-ΔSH2-myc were kind gifts from Kazuo Sugamura, Tohoku University, Sendai, Japan.

Establishment of CD8$^+$ and CD4$^+$ T Cell Lines. The CD8$^+$ or CD4$^+$ T cell lines were established in vitro by stimulating splenocytes from *Gasp*$^{+/+}$ and *Gasp*$^{-/-}$ mice after depleting CD4$^+$ or CD8$^+$ cells, with BALB/c (allogeneic) splenocytes or syngeneic splenocytes in the presence of 2C11 (1 μg/mL). T cell lines were maintained by biweekly stimulations in complete DMEM supplemented with 10% prescreened FCS and 5% conditioned medium that was prepared from culture supernatant of rat splenocytes stimulated with Con A for 48 h.

Cell-Mediated Lymphocytotoxicity Assay. Graded numbers of anti-H-2^d CD8$^+$ T cells were incubated with 5,000 ^{51}Cr-labeled P815 (H-2^d mastcytoma) or EL4 (H-2^b T lymphoma) for 4 h. The supernatants were harvested with the Skatron harvesting system, and radioactivities in the supernatants were measured with a gamma counter. Assays were performed in triplicate.

Cell Stimulation Assays. CD4CD8 DP thymocytes were sorted (FACSAria II; Becton Dickinson) and stimulated with soluble or plate-bound anti-CD3 (clone 2C11) and anti-CD28 antibody each at 5 μg/mL for the indicated times. After 24 h of stimulation IL-2 production was measured in supernatant by mouse IL-2 ELISA Ready-SET-Go! (Ebioscience). Analysis of pERK used CD3 or CD3+CD28 at 5 μg/mL and goat anti-hamster (GAH) Ab at 40 μg/mL.

Ca^{2+} Mobilization Measurements. Sorted CD4CD8 DP cells were labeled with 3 μM Fura2-AM (Molecular Probes/Invitrogen) for 1 h at 37 °C. Cells were washed with ice-cold PBS and resuspended in Ringer's solution. Five million cells were surface-labeled with CD3 or CD3 + 28 at 5 μg/mL on ice for 20 min. Labeled cells were washed and warmed up for 5 min in a cuvette, then cross-linked with 40 μg/mL GAH and analyzed with a fluorescence spectrophotometer (Hitachi F-2500) for fluorescence intensity every 10 s for up to 10 min.

BrdU Administration and FACS Analysis. Mice were fed 0.8 mg/mL BrdU (Nacalai Tesque) for 5 days in drinking water. Antibodies used for staining were phycoerythrin (PE)-antiCD4 (GK1.5; Ebioscience), allophycocyanin (APC)-antiCD8 (53–6.7; Biolegend), and FITC-antiBrdu (3D4; BD Pharmingen). Cells were isolated from spleens and mLN, surface-stained for CD4-PE and CD8-APC, and stained for BrdU incorporation as described (39).

ACKNOWLEDGMENTS. We thank Meiko Fujino and Meiko Takeshita for expert technical assistance; Makoto Koyanagi, Taeko Dohi, Shigeyuki Kano, and Hiroki Aoki for technical advice; Nobukata Shinohara for support; Nobuko Saito, Yusuke Matsuoka, and Tohru Miyoshi-Akiyama for expertise in antibody production; and Shigeo Koyasu for critical reading of the manuscript. This work was supported by Grant-in-Aid for Scientific Research in Priority Areas 20060039 from the Ministry of Education, Culture, Sports, Science, and Technology of Japan.

1. Rothenberg EV, Taghon T (2005) Molecular genetics of T cell development. *Annu Rev Immunol* 23:601–649.
2. Suzuki H, Punt JA, Granger LG, Singer A (1995) Asymmetric signaling requirements for thymocyte commitment to the CD4$^+$ versus CD8$^+$ T cell lineages: A new perspective on thymic commitment and selection. *Immunity* 2:413–425.
3. Starr TK, Jameson SC, Hogquist KA (2003) Positive and negative selection of T cells. *Annu Rev Immunol* 21:139–176.
4. Germain RN (2003) Ligand-dependent regulation of T cell development and activation. *Immunol Res* 27:277–286.
5. Alberola-Ila J, Hernandez-Hoyos G (2003) The Ras/MAPK cascade and the control of positive selection. *Immunol Rev* 191:79–96.
6. Rincon M, Flavell RA, Davis RA (2000) The JNK and P38 MAP kinase signaling pathways in T cell-mediated immune responses. *Free Radical Biol Med* 28:1328–1337.
7. Dower NA, et al. (2000) RasGRP is essential for mouse thymocyte differentiation and TCR signaling. *Nat Immunol* 1:317–321.
8. Gong Q, et al. (2001) Disruption of T cell signaling networks and development by Grb2 haploid insufficiency. *Nat Immunol* 2:29–36.
9. Miosge L, Zamoyska R (2007) Signaling in T cell development: Is it all location, location, location? *Curr Opin Immunol* 19:194–199.
10. Daniels MA, et al. (2006) Thymic selection threshold defined by compartmentalization of Ras/MAPK signaling. *Nature* 444:724–729.
11. Yasuda T, Kurosaki T (2008) Regulation of lymphocyte fate by Ras/ERK signals. *Cell Cycle* 7:3634–3640.
12. Marson A, et al. (2007) Foxp3 occupancy and regulation of key target genes during T cell stimulation. *Nature* 445:931–935.
13. Kaye J, Ellenberger DL (1992) Differentiation of an immature T cell line. A model of thymic-positive selection. *Cell* 71:423–435.
14. Kisielow P, Teh HS, Bluthmann H, von Boehmer H (1988) Positive selection of antigen-specific T cells in thymus by restricting MHC molecules. *Nature* 335:730–733.
15. Park JH, et al. (2007) Coreceptor tuning: Cytokine signals transcriptionally tailor CD8 coreceptor expression to the self-specificity of the TCR. *Nat Immunol* 8:1049–1059.
16. Yamada T, et al. (1991) Inheritance of T helper immunodeficiency (thid) in LEC mutant rats. *Immunogenetics* 33:216–219.
17. Jung CG, Miyamoto T, Tsumagari T, Agui T (2001) Genetic association between low expression phenotype of CD62L (L-selectin) in peripheral CD4$^+$ T cells and the thid (T-helper immunodeficiency) phenotype in the LEC rat. *Exp Anim* 50:337–340.
18. Asano A, Tsubomatsu K, Jung CG, Sasaki N, Agui T (2007) A deletion mutation of the protein tyrosine phosphatase κ (Ptprk) gene is responsible for T-helper immunodeficiency (thid) in the LEC rat. *Mamm Genome* 18:779–786.
19. Kose H, et al. (2007) Maturational arrest of thymocyte development is caused by a deletion in the receptor-like protein tyrosine phosphatase κ gene in LEC rats. *Genomics* 89:673–677.
20. Natsume T, et al. (2002) A direct nanoflow liquid chromatography–tandem mass spectrometry system for interaction proteomics. *Anal Chem* 74:4725–4733.
21. Chardin P, Cussac D, Maignan S, Ducruix A (1995) The Grb2 adaptor. *FEBS Lett* 369:47–51.
22. Egan SE, et al. (1993) Association of Sos Ras exchange protein with Grb2 is implicated in tyrosine kinase signal transduction and transformation. *Nature* 363:45–51.
23. Cussac D, Frech M, Chardin P (1994) Binding of the Grb2 SH2 domain to phosphotyrosine motifs does not change the affinity of its SH3 domains for Sos proline-rich motifs. *EMBO J* 13:4011–4021.
24. Fischer AM, Katayama CD, Pages G, Pouyssegur J, Hedrick SM (2005) The role of erk1 and erk2 in multiple stages of T cell development. *Immunity* 23:431–443.
25. Neilson JR, Winslow MM, Hur EM, Crabtree GR (2004) Calcineurin B1 is essential for positive but not negative selection during thymocyte development. *Immunity* 20:255–266.
26. Werlen G, Hausmann B, Palmer E (2000) A motif in the αβ T cell receptor controls positive selection by modulating ERK activity. *Nature* 406:422–426.
27. McCarty N, et al. (2005) Signaling by the kinase MINK is essential in the negative selection of autoreactive thymocytes. *Nat Immunol* 6:65–72.
28. Zhou T, et al. (1996) Inhibition of Nur77/Nurr1 leads to inefficient clonal deletion of self-reactive T cells. *J Exp Med* 183:1879–1892.
29. Takahama Y, Shores EW, Singer A (1992) Negative selection of precursor thymocytes before their differentiation into CD4$^+$CD8$^+$ cells. *Science* 258:653–656.
30. McNeil LK, Starr TK, Hogquist KA (2005) A requirement for sustained ERK signaling during thymocyte positive selection in vivo. *Proc Natl Acad Sci USA* 102:13574–13579.
31. Qian X, et al. (2000) The Sos1 and Sos2 Ras-specific exchange factors: Differences in placental expression and signaling properties. *EMBO J* 19:642–654.
32. Esteban LM, et al. (2000) Ras-guanine nucleotide exchange factor sos2 is dispensable for mouse growth and development. *Mol Cell Biol* 20:6410–6413.
33. Fu G, et al. (2009) Themis controls thymocyte selection through regulation of T cell antigen receptor-mediated signaling. *Nat Immunol* 10:848–856.
34. Johnson AL, et al. (2009) Themis is a member of a new metazoan gene family and is required for the completion of thymocyte positive selection. *Nat Immunol* 10:831–839.
35. Lesourne R, et al. (2009) Themis, a T cell-specific protein important for late thymocyte development. *Nat Immunol* 10:840–847.
36. Yagi T, et al. (1993) A novel ES cell line, TT2, with high germ line-differentiating potency. *Anal Biochem* 214:70–76.
37. Murata T, et al. (2004) *ang* is a novel gene expressed in early neuroectoderm, but its null mutant exhibits no obvious phenotype. *Gene Expr Patterns* 5:171–178.
38. Oda H, et al. (2009) RhoH plays critical roles in Fcε RI-dependent signal transduction in mast cells. *J Immunol* 182:957–962.
39. Tough DF, Sprent J (1994) Turnover of naive- and memory-phenotype T cells. *J Exp Med* 179:1127–1135.
40. Kakugawa K, et al. (2009) A novel gene essential for the development of single positive thymocytes. *Mol Cell Biol* 29:5128–5135.

Immunology Letters 124 (2009) 27–34

Contents lists available at ScienceDirect

Immunology Letters

journal homepage: www.elsevier.com/locate/

Rac GTPases are involved in development, survival and homeostasis of T cells

Yoshinori Sato[a], Hiroyo Oda[a], Michael S. Patrick[a], Yukari Baba[b], Ahmed A. Rus'd[b], Yoshinao Azuma[b], Takaya Abe[c], Mutsunori Shirai[b], Harumi Suzuki[a,*]

[a] Department of Pathology, Research Institute, International Medical Center of Japan, 1-21-1 Toyama, Shinjuku, Tokyo 162-8655, Japan
[b] Department of Microbiology, Yamaguchi University School of Medicine, Ube 755-8685, Japan
[c] Laboratory for Animal Resources and Genetic Engineering, Center for Developmental Biology, RIKEN Kobe, Chuou-ku, Kobe 650-0047, Japan

ARTICLE INFO

Article history:
Received 27 February 2009
Received in revised form 23 March 2009
Accepted 29 March 2009
Available online 5 April 2009

Keywords:
Rac
T cell survival and homeostasis

ABSTRACT

Rac GTPases consist of Rac1, 2 and 3, and each of them have redundant and differential functions. Rac1 is the most ubiquitously and abundantly expressed of the three and has been shown to work as a "molecular switch" in various signal transduction pathways. Although Rac1 and Rac2 are both activated by TCR ligation, little is known about the function of Rac GTPases in the development and activation of T cells. In order to investigate the precise function of Rac GTPases in T cells in vivo, we established dominant negative Rac1 transgenic (dnRac1-Tg) mice controlled by the human CD2 promoter. Total numbers of thymocytes of dnRac1-Tg mice were significantly decreased because of impaired transition from the CD4CD8 double negative stage to the CD4CD8 double positive (DP) stage. Although positive selection of CD4 single positive (SP) was not altered, positive selection of CD8-SP was slightly increased. On the contrary, the number of mature CD4-SP and CD8-SP cells in the spleen, mesenteric lymph nodes and peripheral blood was severely decreased in dnRac1-Tg mice. Proliferation of splenic CD4-SP cells upon TCR stimulation in vitro was unaltered, however, homeostatic proliferation of dnRac1-Tg splenic CD4-SP cells in lymphopenic mice was severely reduced. Finally, we found increased spontaneous apoptosis of DP thymocytes and mature T cells in dnRac1-Tg mice, possibly because of reduced phosphorylation of Akt with or without TCR stimulation. Collectively, the current results indicate that Rac GTPases are important in survival of DP thymocytes and mature T cells in vivo by regulating Akt activation.

1. Introduction

Rac belongs to the Rho family of small guanosinetriphosphatases (GTPases), and is a critical signaling regulator acting as a molecular switch in mammalian cells [1–4]. Rac consists of three independent genes; Rac1 is expressed ubiquitously, Rac2 is expressed only in hematopoietic cells, and Rac3 is expressed mainly in the brain [1–5]. Rac1 regulates various cellular functions such as cellular growth, cytoskeletal rearrangement, and apoptosis [6–8]. Rac2 is important for superoxide production, phagocytosis by neutrophils, regulation of leukocyte lineage differentiation, regulation of B cell adhesion and immunological-synapse formation [9–11]. Rac3 is relevant to later events in the development of a functional nervous system [12]. Because Rac1 deficient mice die in utero [13], a conditional knockout strategy was applied for the analysis of its function. Distinct and critical roles of Rac1 and Rac2 in growth and engraftment of hematopoietic stem cells [5,14,15] as well as in B cell development [16] were reported by using conditional knockout mice for Rac1 on a $Rac2^{-/-}$ background.

However, little is known about the function of Rac GTPases in T cell development and activation. Rac2-deficient mice showed normal T cell development in the thymus, defective Th1 differentiation caused by decreased IFN-γ production [17], perturbed chemotaxis [18], and defective T cell activation accompanied by decreased ERK activation [19]. Overexpression of constitutively active mutants of Rac1 (L61Rac1 and L61Y40CRac1) induced pre-T cell differentiation and proliferation on a $RAG^{-/-}$ background [20], and conversion of positive selection to negative selection in the thymus [21]. The results indicates that Rac1 regulates the strength of TCR-mediated signal transduction. Very recently, mice with conditional disruption of both Rac1 and Rac2 in the thymus were reported and they showed reduced development of T cell and impaired activation with increased cell death [22,23].

Although Rac1 and Rac2 are abundantly expressed in the thymus, we found that Rac3 too was weakly expressed in the thymus. Because all three Rac GTPases are expressed in the thymus, we decided to establish transgenic mice with thymocyte-specific expression of a dominant negative mutant form of Rac1

* Corresponding author. Tel.: +81 3 3232 3100; fax: +81 3 3232 3100.
E-mail address: hsuzuki@ri.imcj.go.jp (H. Suzuki).

0165-2478/$ – see front matter © 2009 Elsevier B.V. All rights reserved.
doi:10.1016/j.imlet.2009.03.014

(N17 mutation), which is known to inhibit all three Rac GTPases [24]. Overexpression of the dominant negative (dn) Rac1N17 mutant cDNA in a T cell line successfully inhibited TCR/CD28-dependent Rac signaling downstream of Vav [25,26]. In the current study, dnRac1 transgenic (Tg) mice whose expression is controlled by human CD2 promoter showed impaired β-selection in the thymus and decreased numbers of peripheral mature T cells. TCR-stimulated proliferation of dnRac1-expressing T cells in vitro was not affected, but homeostatic proliferation of mature T cells was significantly decreased. Spontaneous apoptosis as well as TCR-induced apoptosis of T cells were increased with defective phosphorylation of Akt. These results indicate that Rac GTPases are important in proliferation, survival and homeostasis of T cells.

2. Materials and methods

2.1. Generation of dominant negative Rac1 transgenic mice

Dominant negative (N17) mutant Rac1 cDNA was cloned into the CD2-VA cassette [27] and the construct was microinjected into male pronuclei of C57Bl/6 fertilized eggs to establish transgenic mouse lines (hCD2-dnRac1-LCR transgenic mice: Acc. No. CDB0448T; http://www.cdb.riken.jp/arg/mutant%20mice%20list.html). Four different transgene-expressing lines were obtained and line#22 which showed the highest expression was used in the current study. The experiments described in this study were performed in adherence to institutional ethical guidelines for animal experiments and safety guidelines for gene manipulation experiments. Approval by the Animal Use Committee of the Research Institute of International Medical Center of Japan was obtained before the start of the experiments.

2.2. FACS analysis and antibodies

Thymocytes and peripheral T cells were stained with various combinations of FITC-conjugated anti-CD8 (53-6.7), anti-CD45.2 (Clone 104), PE-conjugated anti-CD4 (GK1.5), biotin-conjugated anti-TCRβ (597-H57), anti-CD5 (53-7.3) antibodies and Annexin V. Stained cells were analyzed on a Becton Dickinson FACScan flow cytometer using CellQuest software.

2.3. TCR-stimulation of thymocytes and splenic CD4-SP T cells

CD4-SP T cells were isolated by MACS using biotin-conjugated anti-CD4 antibody and streptavidin microbeads (Miltenyi Biotec). Freshly isolated thymocytes and CD4-SP splenocytes were incubated with anti-CD3 and anti-CD28 mAb (10 μg/ml each) for 20 min on ice and washed by ice-cold PBS followed by goat antihamster polyclonal antibody (40 μg/ml, Jackson ImmunoResearch Lab, West Grove, PA) and incubated for 2 or 5 min at 37 °C. Thymocytes and splenic CD4-SP T cells were lysed and analyzed by SDS-PAGE. Transferred membranes were Western-blotted with following the antibodies, anti-phopho-Erk, anti-Erk, anti-phospho-Akt (Ser473) and anti-Akt antibodies (Cell Signaling Technology, Beverly, MA). Detected proteins were visualized with ECL chemiluminescent substrate (Cell Signaling Technology).

2.4. Active Rac pull-down assay

Activity of Rac GTPases was measured by the standard p21-activated kinase (PAK)-binding domain assay. After 2×10^7 thymocytes were stimulated by TCR crosslinkimg, activated Rac protein was precipitated with p21-binding domain (PBD) beads (Upstate Biotechnology, Lake Placid, NY) and subjected to Western blotting analysis using Rac1- (23A8, Upstate Biotechnology), Rac2- (sc-96, Santa Cruz Biotechnology) or Rac3- [28] specific antibodies.

2.5. Labeling of CD4-SP T cells

CD4-SP T cells were labeled with 5(6-) Carboxyfluorescein diacetate N-succinimidyl ester (CFSE, Sigma, St. Louis, MO). Briefly, CD4-SP T cells isolated from spleen by MACS were resuspended at a concentration of 1×10^7 cells/ml in 5% FCS/PBS. Final concentration of 5 μM CFSE was added to the cell suspension. After a 5 min incubation period at 25 C, the excess CFSE was washed by adding 5% FCS/PBS, and then resuspended in RPMI1640 containing 10% FCS.

2.6. Measurement of T cell growth in vitro

For proliferation assays, 96-well plates were coated with 0.1 ml of purified anti-CD3 (5 μg/ml) and anti-CD28 antibodies (5 μg/ml), and CFSE-labeled CD4-SP T cells were plated at a density of 2×10^5 cells and the culture was continued for 3 days at 37 C. After incubation, CD4-SP T cells were analyzed on FACScan flow cytometor. For MTT assays, CellTiter 96® AQueous One Solution Cell Proliferation Assay kit (Promega, Madison, WI) was used. For survival assays, T cells were plated at a density of 1×10^6 cells/well in 96-well plates with or without 1 ng/ml IL-7 in a final volume of 200 μl/well.

2.7. Homeostatic proliferation analysis

Purified splenic CD4-SP T cells (2×10^6) from dnRac1-Tg or littermate control mice were injected into CD45.1, $RAG^{-/-}$ mice. Fourty days later, spleen, mesenteric lymph node and peripheral blood were harvested and cells were analyzed by FACS using, anti-CD45.2, anti-CD4 and anti-TCRβ antibodies.

2.8. Statistical analysis

Results are expressed as the mean ± S.E.M. of three independent experiments performed in triplicate. Student's *t*-test was used for multiple comparisons, and differences were considered to be statistically significant when the *p*-value was less than 0.05 or 0.01.

3. Results

3.1. Impaired differentiation of DP thymocytes in thymi of dnRac1-Tg mice

Both Rac1 and Rac2 are expressed in the thymus [1,20], however, expression of Rac3 in the thymus has not been characterized yet. We found low expression of Rac3 in the thymus by RT-PCR (Fig. 1A). However, we could not detect Rac3 protein by Western blotting using Rac3 specific antisera [28] (data not shown). Therefore, major Rac GTPases functioning in the thymus are Rac1 and Rac2. To investigate the precise function of Rac GTPases in T cell development and activation, we employed a dominant negative strategy which can suppress all three Rac GTPases [24]. We established dominant negative Rac1 transgenic (dnRac1-Tg) mice controlled by the human CD2 promoter containing the locus control region [29]. Expression of introduced HA-tagged dnRac1(N17) protein in the thymus of transgenic mice was detected as an upper band in Fig. 1B, which is also confirmed by Western blotting with anti-HA antibody (data not shown). As expected, TCR-induced activation of both Rac1 and Rac2 in dnRac1-Tg DP thymocytes was significantly inhibited (Fig. 1C).

The total number of thymocytes in dnRac1-Tg mice was decreased compared to littermate controls ($2.2 \pm 0.2 \times 10^8$ cells for controls; $1.5 \pm 0.1 \times 10^8$ cells for dnRac1-Tg). In dnRac1-Tg mice,